Chapter 9B. Analysis of Imaging Spectrometer Data for the Kharnak-Kanjar Area of Interest

By Raymond F. Kokaly and Michaela R. Johnson

Abstract

Imaging spectrometer data collected over the Kharnak-Kanjar area of interest (AOI) in central Afghanistan were analyzed with spectroscopic methods to identify the occurrence of selected material classes at the surface. Absorption features in the spectra of HyMap data were compared to a reference library of spectra for known materials. The mineral found most frequently in the Kharnak-Kanjar AOI was calcite. Significant areas were also found to contain calcite mixed with muscovite or clay classes. However, pixels with the best match to muscovite or illite spectra were also identified over large contiguous areas in the southeastern and northwestern portions of the AOI. In general, pixels in polygons of the younger Early Cretaceous rocks in the Barremian-Aptian category were identified as matching the pure calcite spectra of the calcite and calcite-abundant classes. In contrast, polygons of the Berriasian-Valanginian category of Early Cretaceous rocks had very little of their area mapped in the pure calcite classes; most of the area of these polygons were matched to classes containing muscovite or illite. The Valanginian-Hauterivian category had intermediate composition; polygons of this unit contained some pixels with strong calcite absorption features, but more often the spectra of pixels in this category were matched to kaolinite mixed with calcite (in the eastern part of the AOI) or to calcite mixed with muscovite or clay (in the western part of the AOI). Epidote and chlorite were present in spatially consistent patterns in the southeastern part of the AOI, along the southern boundary of the AOI, and in and around the intrusive rocks near the western boundary of the AOI. Two minerals, buddingtonite and pyrophyllite, that can be formed hydrothermally and are possible indicators of mercury, gold, or silver deposits, were found. Buddingtonite was detected in a mapped unit of Valanginian-Hauterivian Early Cretaceous rocks, with the kaolinite and alunite detected along the contact with Pliocene rocks nearby. An extensive area of pixels matching the spectrum of pyrophyllite, a phyllosilicate that can be formed hydrothermally and is a possible indicator of gold and silver deposits, was present extending more than 13 kilometers in length and up to 7 kilometers in width, within a mapped unit of Valanginian-Hauterivian Early Cretaceous rocks. The minerals detected in the HyMap imaging spectrometer around the known mercury occurrences were in good agreement with the descriptions of Abdullah and others (1977) for mercury occurrences as having a stock consisting mainly of calcareous-dickitized metasomatites having variable iron hydroxide content. Patterns of kaolinite mixed with calcite and calcite mixed with clay/muscovite, within areas mapped as containing goethite and surrounded by areas containing just calcite, are present close to the Kharnak, Pushwara, Duwalak and Surkhnow mineral occurrences in the Koh-e-Katif Passaband subarea; the Khanjar, Qalat, Alibali, Alibali-I, Alibali-II, Gulgadam, and Sahebdad occurrences in the Sahebdad Khanjar subarea; and the Mullayan occurrence in the Pahjshah Mullayan subarea. In all subareas, additional sites with mineral patterns similar to those near mercury occurrences were present distant from the known mineral occurrences. In future studies of the Kharnak-Kanjar AOI, these locations should be included as potential field sampling sites.

9B.1 Introduction

Past studies of geologic data of Afghanistan revealed numerous areas with indications of potential mineral resources of various types (Peters and others, 2007; Abdullah and others, 1977). Several of these potential mineral resource areas were selected for follow-on studies using imaging

spectroscopy to characterize surface materials. Imaging spectroscopy is an advanced type of remote sensing also known as hyperspectral remote sensing. One of the selected areas is the Kharnak-Kanjar area of interest (AOI) in central Afghanistan, which is approximately 400 kilometers (km) west of Kabul (fig. 9B–1). The area is believed to have the potential for mercury and gold. To help assess these potential resources, high resolution imaging spectrometer data were analyzed to detect the presence of selected minerals that may be indicative of past mineralization processes. This report contains the results of spectroscopic analyses and identifies sites within the Kharnak-Kanjar AOI that deserve further investigation, especially detailed geologic mapping, lithologic sampling, and geochemical studies.

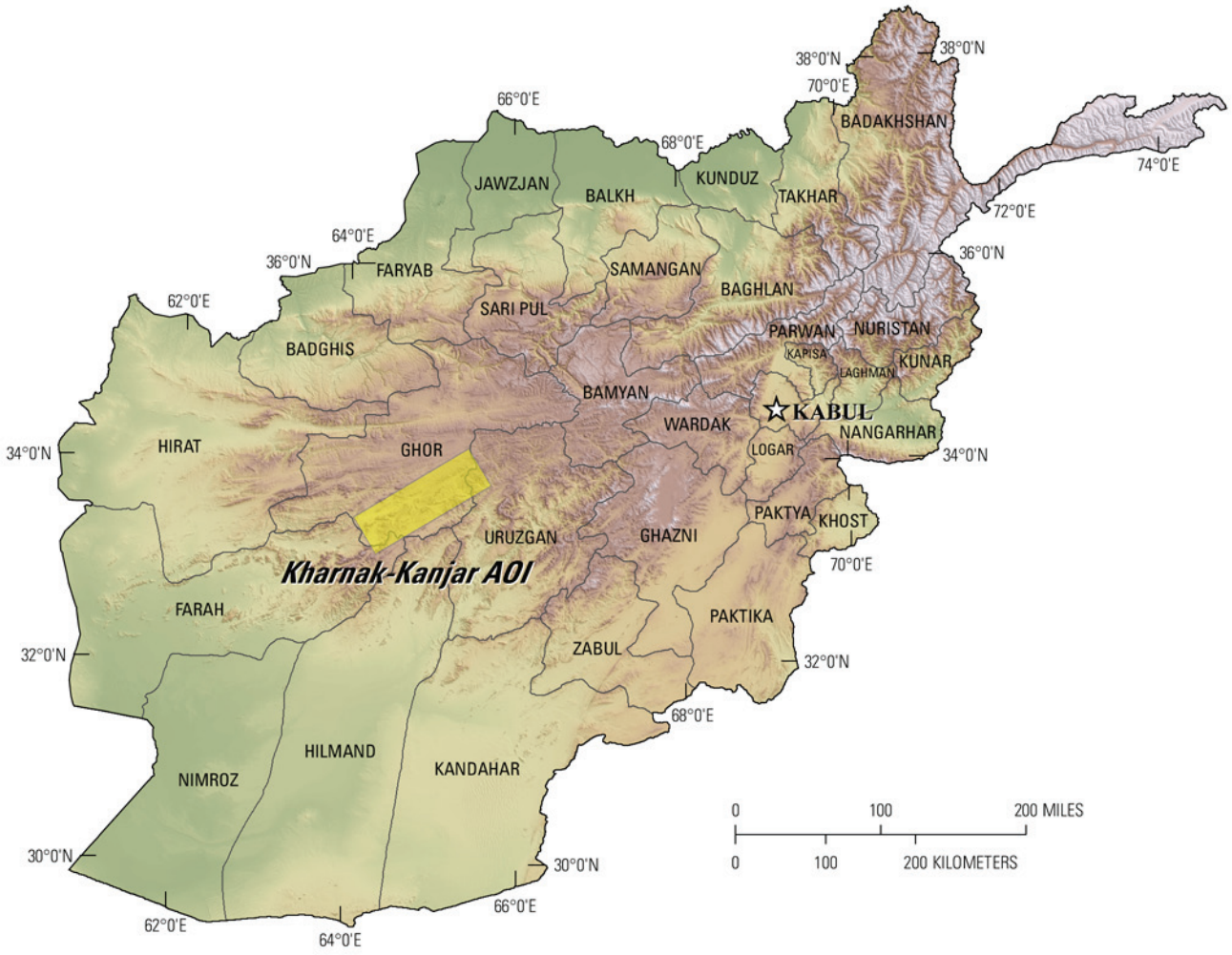

Figure 9B–1. Index map of the Kharnak-Kanjar area of interest, central Afghanistan.

9B.2 Data Collection and Processing

In 2007, imaging spectrometer data were acquired over most of Afghanistan as part of the U.S. Geological Survey (USGS) oil and gas resources assessment of the Katawaz and Helmand Basins project. These data were collected to characterize surface materials in support of assessments of resources (coal, water, minerals, and oil and gas) and earthquake hazards in the country (King and others, 2010). Imaging spectrometers measure the reflectance of visible and near-infrared light from the Earth's surface in many narrow channels, producing a reflectance spectrum for each image pixel. These reflectance spectra can be interpreted to identify absorption features that arise from specific chemical transitions and molecular bonds that provide compositional information about surface materials. Imaging spectrometer data can only be used to characterize the surface materials and not subsurface composition

or structure. Subsurface processes can be indicated, however, by the distribution of surface materials that can be detected using imaging spectroscopy data.

9B.2.1 Collection of Imaging Spectrometer Data

The HyMap imaging spectrometer (Cocks and others, 1998) was flown over Afghanistan from August 22 to October 2, 2007 (Kokaly and others, 2008). HyMap has 512 cross-track pixels and covers the wavelength range from 0.43 to 2.48 microns (μm) in 128 channels. The imaging spectrometer was flown on a WB–57 high altitude aircraft at approximately 50,000 feet (ft). There were 207 standard data flight lines and 11 cross-cutting calibration lines collected over the country of Afghanistan for a total of 218 flight lines, covering a surface area of 438,012 square kilometers (km^2) (Kokaly and others, 2008). Data were received in scaled radiance form (calibrated to National Institute of Standards and Technology reference materials). Before processing, four channels that had low signal-to-noise ratios and (or) were in wavelength regions overlapped by adjacent detectors were removed from the image cubes. Each flight line was georeferenced to Landsat base imagery in Universal Transverse Mercator (UTM) projection (Davis, 2007).

9B.2.2 Calibration Process

HyMap data were converted from radiance to reflectance using a multistep calibration process. This procedure removed the influence of the solar irradiance function, atmospheric absorptions, and residual instrument artifacts, resulting in reflectance spectra that have spectral features that arise from the material composition of the surface. Because of the extreme topographic relief and restricted access to ground calibration sites, modifications to the standard USGS calibration procedures were required to calibrate the 2007 Afghanistan HyMap dataset (Hoefen and others, 2010). In the first step of the calibration process, the radiance data were converted to apparent surface reflectance using the radiative transfer correction program Atmospheric CORrection Now (ACORN; ImSpec LLC, Palmdale, Calif.). The ACORN program was run multiple times for each flight line, using average elevations in 100-meter (m) increments, covering the range of minimum to maximum elevations encountered within the flight line. A single atmospherically corrected image was assembled from these elevation-incremented ACORN results by determining the elevation of each HyMap pixel and selecting the atmospherically corrected pixel from the 100-m increment closest to that elevation.

Each assembled atmospherically corrected image was further empirically adjusted using ground-based reflectance measurements from a ground calibration site. Five ground calibration spectra were collected in Afghanistan: Kandahar Air Field, Bagram Air Base, and Mazar-e-Sharif Airport, as well as soil samples from two fallow fields in Kabul. At each site, the average field spectrum of the ground target was used to calculate an empirical correction factor using the pixels of atmospherically corrected HyMap data in the flight lines that passed over the site. Subsequently, each of the HyMap flight lines was ground-calibrated using the empirical correction from the closest calibration site.

To further improve the data quality, an additional calibration step was taken to address the atmospheric differences caused, in part, by the large distances between the calibration sites and the survey areas. The large distances were the result of a lack of safe access to ground calibration sites. The duration of the airborne survey and variation in time of day during which flight lines were acquired also resulted in differences in atmospheric conditions between standard flight lines and lines over ground calibration sites, which were used to derive the empirical correction factors. Over the course of the data collection process, the sun angle, atmospheric water vapor, and atmospheric scattering differed for each flight line. To compensate for this variation, cross-cutting calibration flight lines over the ground calibration areas were acquired (Kokaly and others, 2008) and used to refine the reflectance calculation for standard data lines. A multiplier correction for standard data lines, typically oriented as north-south flight lines, was derived using the pixels of overlap with the well-calibrated cross-cutting lines, subject

to slope, vegetation cover, and other restrictions on pixel selection (Hoefen and others, 2010). As a result, the localized cross-calibration multiplier, derived from the region of overlap, reduced residual atmospheric contamination in the imaging spectrometer data that may have been present after the ground calibration step.

9B.2.3 Materials Maps and Presentation

After the calibration process, the georeferenced and calibrated reflectance data were processed. The reflectance spectrum of each pixel of HyMap data was compared to the spectral features of reference entries in a spectral library of minerals, vegetation, water, and other materials (King and others, 2011; Kokaly and others, 2011). The best spectral matches were determined for each pixel, and the results were clustered into classes of materials discussed next.

HyMap reflectance data were processed using MICA (Material Identification and Characterization Algorithm), a module of the U.S. Geological Survey PRISM (Processing Routines in IDL for Spectroscopic Measurements) software (Kokaly, 2011). The MICA analysis compared the reflectance spectrum of each pixel of HyMap data to entries in a reference spectral library of minerals, vegetation, water, and other materials. The HyMap data were compared to 97 reference spectra of well-characterized mineral and material standards. The resulting maps of material distribution, resampled to 23 × 23-m square pixel grid, were mosaicked to create thematic maps of surface mineral occurrences over the full dataset covering Afghanistan.

The MICA module was applied to HyMap data twice to present the distribution of two categories of minerals naturally separated in the wavelength regions of their primary absorption features. MICA was applied using the subset of minerals with absorption features in (1) the visible and near-infrared wavelength region, producing the 1-micrometer (μm) map of iron-bearing minerals and other materials (King and others, 2011), and (2) the shortwave infrared region to produce the 2-μm map of carbonates, phyllosilicates, sulfates, altered minerals, and other materials. For clarity of presentation, some individual classes in these two maps were bundled by combining selected mineral types (for example, all montmorillonites or all kaolinites) and representing them with the same color in order to reduce the number of mineral classes.

The iron-bearing minerals analysis includes 28 classes. Iron-bearing minerals with different mineral compositions but similar broad spectral features are difficult to classify as specific mineral species. Thus, generic spectral classes, including several minerals with similar absorption features, such as Fe^{3+} Type 1 and Fe^{3+} Type 2, are depicted on the map. The carbonates, phyllosilicates, sulfates, and altered minerals analysis includes 32 classes. Minerals with slightly different compositions but similar spectral features are less easily distinguished; therefore, some identified classes consist of several minerals with similar spectra, such as the "chlorite or epidote" class. When comparisons with reference spectra provided no viable match, a designation of "not classified" was assigned to a pixel.

9B.3 Geologic Setting of the Kharnak-Kanjar Area of Interest

The Kharnak-Kanjar AOI is mainly within the Ghor Province in central Afghanistan, with the northeastern part located within Uruzgan province and the southwest part located within Farah province. The contrast-enhanced stretch of the natural-color composite of Landsat Thematic Mapper bands in figure 9B–2 provides a general overview of the Kharnak-Kanjar AOI terrain, and is useful for understanding the general characteristics and distribution of surficial material, including rocks and soil, unconsolidated sediments, vegetation, and hydrologic features.

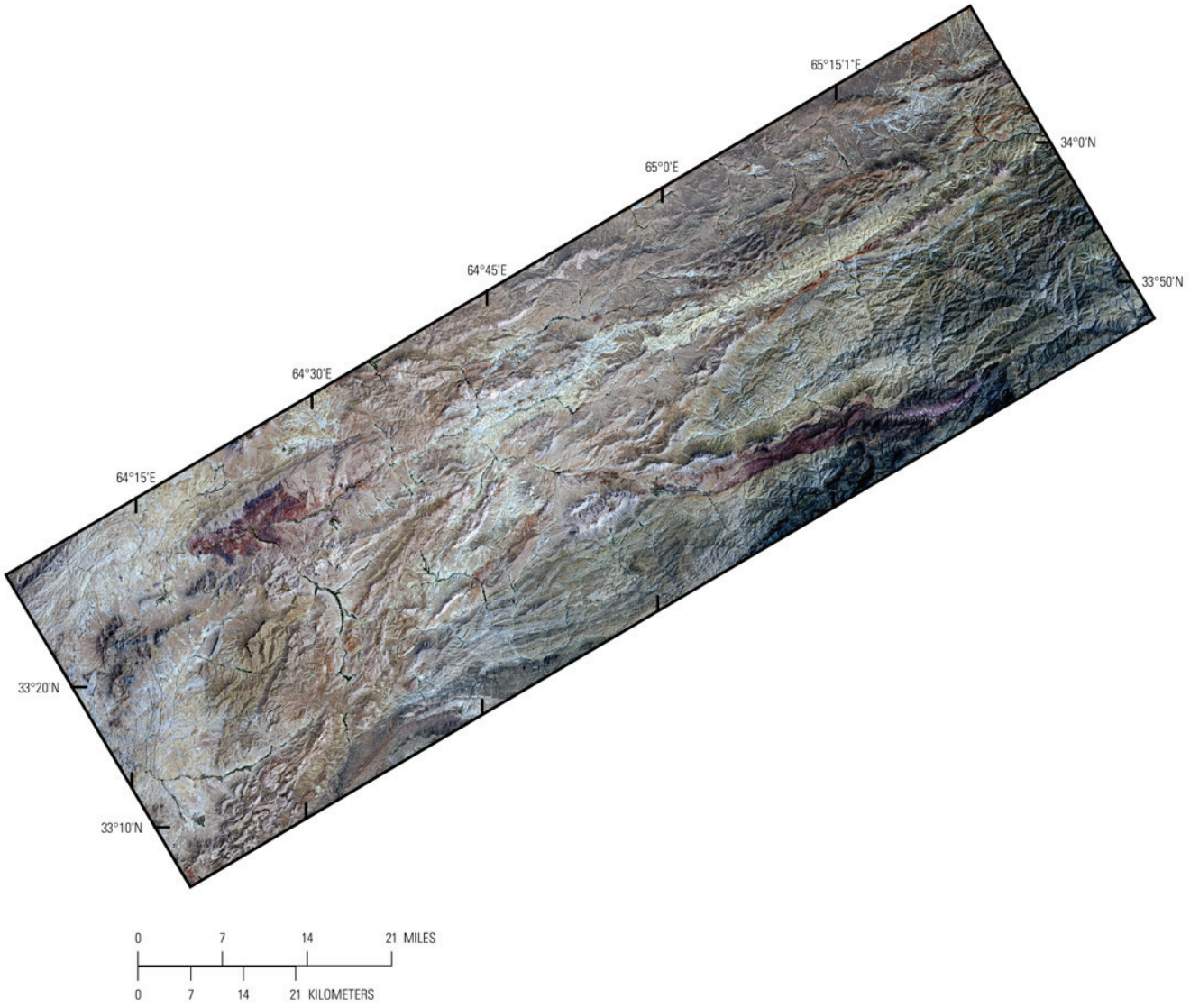

Figure 9B–2. Landsat Thematic Mapper natural color image, contrast enhanced, of the Kharnak-Kanjar area of interest.

9B.3.1 Topography

Elevations in the Kharnak-Kanjar AOI range between 1,853 and 3,869 m (fig. 9B–3). The highest areas are in the northeastern corner of the Kharnak-Kanjar AOI, in sharply defined mountain ranges that are typically controlled by faults. The low areas include a long valley in the western part of the AOI that includes the district centers of Pasaband and Taywara. Other populated areas include the towns of Pushwarah in the southwestern portion of the area and Sharaban in the eastern part of the Kharnak-Kanjar AOI.

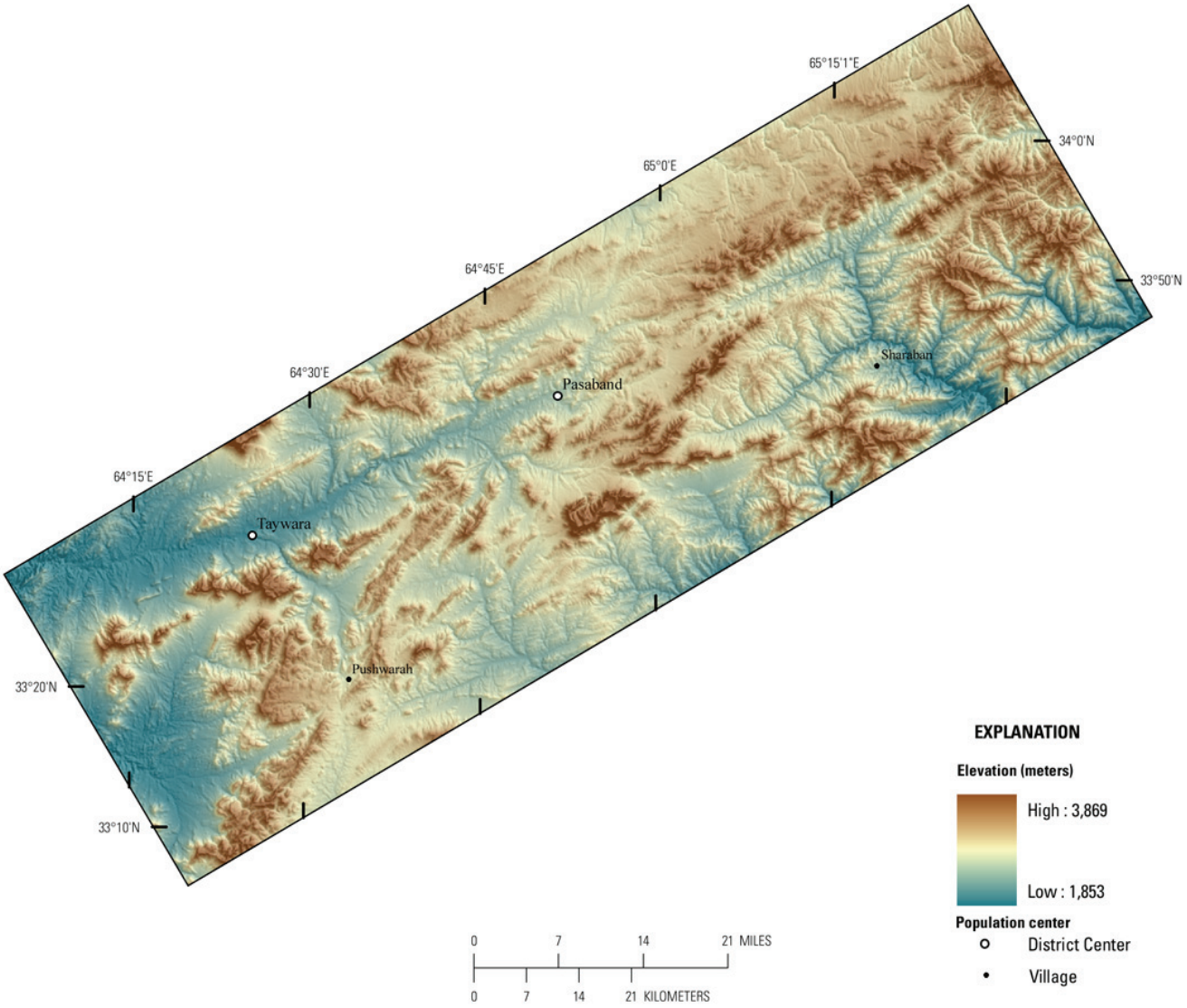

Figure 9B–3. Map showing the range of elevations in the Kharnak-Kanjar area of interest.

9B.3.2 Lithology and Structure

The majority of rocks in the Kharnak-Kanjar AOI are Early Cretaceous sandstone, siltstone, limestone, marl, and conglomerate (fig. 9B–4; Abdullah and Chmyriov, 1977; Doebrich and Wahl, 2006; Peters and others, 2007). The Early Cretaceous rocks are subdivided into Berriasian-Valanginian, Valanginian-Hauterivian, and Barremian-Aptian ages. Older stratified rocks of Late Jurassic-Early Cretaceous age, including shale, siltstone, sandstone, conglomerate, chert, limestone, greenstone, and acidic and mafic volcanic rocks, occur along the southern boundary of the area, in the eastern part of the AOI. Younger Eocene-Oligocene basalt, trachyte, dacite, rhyolite, ignimbrite, tuff, conglomerate, sandstone, siltstone, and limestone crop out in the AOI adjacent to Oligocene sandstone, siltstone, clay, conglomerate, limestone, marl, acidic and mafic volcanic rocks. A relatively small area of Miocene rocks, including redstone, clay, acidic and mafic volcanic rocks, limestone, and marl, is present in the northeastern corner of the AOI. The youngest rocks in the Kharnak-Kanjar AOI are Pliocene gray conglomerate, gravelstone, sandstone, siltstone, clay, limestone, marl, gypsum, salt, and acidic and mafic volcanic rocks.

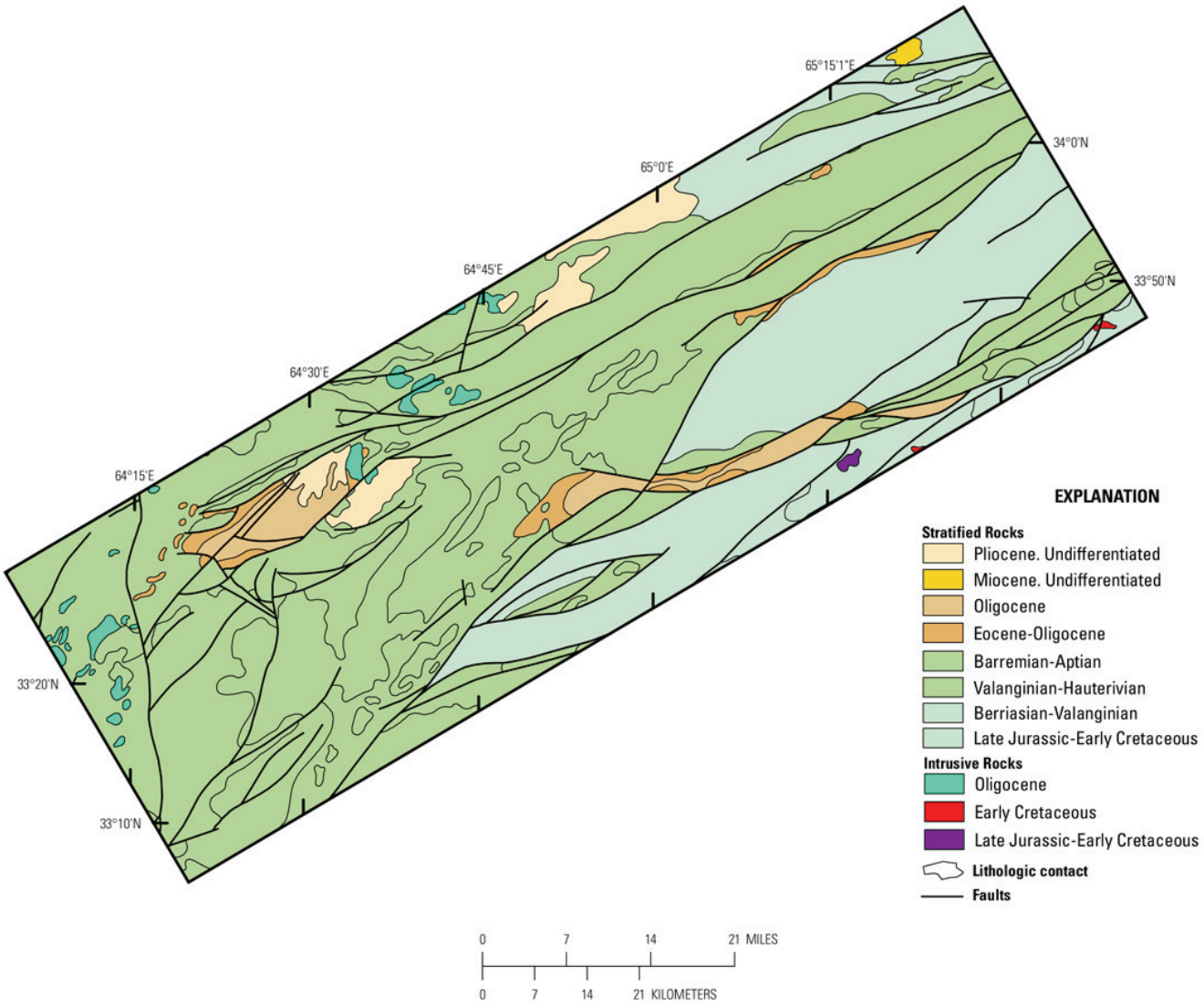

Figure 9B–4. Geologic map of the Kharnak-Kanjar area of interest. Geology from digital geologic map of Afghanistan (Abdullah and Chmyriov, 1977; Doebrich and Wahl, 2006; Peters and others, 2007).

Intrusive rocks cover a small fraction of the AOI. Oligocene intrusive rocks, including granite, granite porphyry, granodiorite, quartz syenite, and granosyenite, occur in a scattered pattern at the western boundary of the AOI. A single small area of Early Cretaceous intrusive rocks, including gabbro, diorite, and plagiogranite, is present in the southeastern corner of the AOI. Late Jurassic-Early Cretaceous diabase and gabbrodiabase rocks occur within stratified rocks of the same age in a small area along the southern boundary of the Kharnak-Kanjar AOI.

9B.3.3 Known Mineralization

Figure 9B–5 shows 20 locations where mineralization with a potential for resource development may exist (Peters and others, 2007). Mercury and copper occurrences have been found within the Kharnak-Kanjar AOI (Abdullah and others, 1977). The characteristics of the mineralized locations are summarized in table 1. The mineral occurrences are divided into three geographic subareas (marked in fig. 9B–5): Koh-e-Katif Passaband, Sahebdad Khanjar, and Pahjshah Mullayan.

Figure 9B–5. Map showing sites of mineralization (Peters and others, 2007) indicated by deposit type on the geologic map of the Kharnak-Kanjar area of interest from digital geologic map of Afghanistan (from Abdullah and Chmyriov, 1977; Doebrich and Wahl, 2006; Peters and others, 2007). unk, unknown.

Table 9B–1. Sites of known mineralization in the Kharnak-Kanjar area of interest.

[Data are from Peters and others (2007). Cu, copper; Pb, lead; Hg, mercury; cm, centimeter; km, kilometer; m, meter; mm, millimeter; km^2, square kilometer]

Name	Deposit type	Major commodity	Deposit size, description	Alteration	Mineralogy	Gangue
Gariba	Skarn Cu	Cu, Pb	Occurrence, thickness: 40 to 60 m; extent: 3 km	Skarn alteration	Chalcopyrite; galena; sphalerite; pyrite	No data.
Pushwara	Unknown Hg	Hg	Occurrence, width: up to 0.7 km; area: occasionally 1.5 km^2	Dickitization; carbonatization	Cinnabar	Dickite; carbonate.
Unnamed	Unknown Hg	Hg	Showing, thickness: 2 to 8 m; extent: 25 to 60 m	Carbonate-dickite alteration	Cinnabar	Dickite; carbonate.
Qasem	Unknown Hg	Hg	Occurrence, area: from 1×3 up to 20×100 m	Dickitization; carbonatization	Cinnabar	Dickite; carbonate.
Mullayan	Unknown Hg	Hg	Occurrence, area: 3.5×2 m (up to 9 m); extent: 200 m	Argillic alteration of quartz-dickite facies; dickitization; silicification; calcite alteration	Cinnabar; pyrite; chalcopyrite; sphalerite; metacinnabarite; arsenopyrite; antimonite; realgar	Dickite; calcite; quartz; ankerite; siderite; barite.
Koh-i-Katif	Unknown Hg	Hg	Occurrence, area: 1000 sq. m	Dickitization; carbonatization	Cinnabar	Dickite; carbonate.
Panjshah	Unknown Hg	Hg	Occurrence	Dickitization; carbonatization	Cinnabar; metacinnabarite; pyrite; hematite; chalcopyrite	Quartz; dickite; calcite; siderite; ankerite; barite.
Katif	Unknown Hg	Hg	Occurrence, thickness: 10 to 20 m; extent: 100 to 150 m; thickness: up to 1.5 cm; ore lodes extent: 43 m; thickness: 1 m	Calcite alteration; dickitization	Cinnabar	Dickite; calcite.
Duwalak	Unknown Hg	Hg	Occurrence, width: 10 to 160 m; extent: 0.75 to 1 km; thickness: 4 to 6 m; extent: 40 to 140 m	Dickitization; carbonatization; limonitization	Cinnabar	Dickite; carbonate; limonite.
Kharnak	Unknown Hg	Hg	Occurrence, extent: 140 to 180 m; thickness: 1 to 24 m; thickness: 1 to 5 m; extent: 20 to 100 m	Carbonate-dickite alteration; dickitization; carbonatization	Cinnabar	Dickite; carbonate.
Surkhnow	Unknown Hg	Hg	Occurrence, area: up to 0.01 km^2; width: 100 to 400 m; extent: more than 2 km.	Carbonatization; dickitization; limonitization	Cinnabar	Dickite; carbonate.
Sebak	Unknown Hg	Hg	Occurrence, width: 0.4 km	Carbonatization; dickitization	Cinnabar	Dickite; carbonate.
Pasaband	Unknown Hg	Hg	Occurrence, thickness: 3 to 8 m; extent: 400 m	Hornfels; dickitization; carbonatization	Cinnabar; realgar; sulfur native; pyrite; hematite	Calcite; ankerite; siderite; dickite; carbonate.
Qalat	Unknown Hg	Hg	Occurrence, extent: 145 to 300 m; thickness: 3 to 22 m	Dickite-carbonate alteration; quartz-dickite-carbonate alteration	Cinnabar; pyrite; arsenopyrite; realgar	Dickite; barite; calcite; gypsum.
Sahebdad	Unknown Hg	Hg	Occurrence, area: 10–20×160 m	Dickitization; carbonatization	Cinnabar; pyrite; chalcopyrite; sphalerite; metacinnabarite; arsenopyrite; antimonite; realgar	Dickite; calcite; quartz; ankerite; siderite; barite.
Gulgadam	Unknown Hg	Hg	Occurrence, extent: 150–170 m; thickness: 3 to 8 m	Carbonatization; dickitization	Cinnabar	Calcite.

Name	Deposit type	Major commodity	Deposit size, description	Alteration	Mineralogy	Gangue
Alibali I	Unknown Hg	Hg	Occurrence, extent: 250–530 m; thickness: 5.4 m; thickness: 1–4 mm	Carbonatization; dickitization	Cinnabar	Dickite; carbonate.
Alibali II	Unknown Hg	Hg	Occurrence, extent: more than 1 km; width: 0.1 to 0.25 km; thickness: 0.05 to 0.2 m	No data	Cinnabar	No data.
Alibali	Unknown Hg	Hg	No data	No data	No data	No data.
Khanjar	Unknown Hg	Hg	Occurrence, thickness: 2 to 4 m; extent: more than 1 km	Carbonatization; dickitization; limonitization	Cinnabar	Dickite; calcite; limonite.

Generally, the mercury occurrences are described by Abdullah and others (1977) as occurring in Early Cretaceous deposits, which are faulted and intruded by diorite porphyrite dikes. Mercury mineralization is associated with zones of hornfelsed, limonitized, dickitized, or carbonatized breccia and sandstone. The presence of cinnabar is noted in some of these occurrences.

The nine mineral occurrences in the Koh-e-Katif Passaband subarea include Kharnak, Koh-e-Katif, Pasaband, Pushwara, Sebak, Qasem, Surkhnow, Katif, and Duwalak. These mineral occurrences are described by described by Abdullah and others (1977). Kharnak is in the vicinity of abundant ancient workings. The Kharnak mineral occurrence is an area of intrusive stock 500 m long by 100 to 170 m wide; the occurrence includes strongly altered stock that consists mainly of calcareous-dickitized metasomatites containing 0.10 to 3.2 percent mercury. Pushwara is also a fairly large occurrence, described as covering a 1.5-km^2 area. Duwalak is described as two mineralized zones, namely, the eastern and western. The Duwalak Eastern Zone measures 10 to 30 m in width, 1 km in length, containing 0.2 to 0.7 percent mercury. The Duwalak Western Zone ranges between 75 and 160 m in width and is 750 m long, with up to 0.14 percent mercury. In the Katif occurrence, mineralized zones range between 10 and 20 m in width and 100 and 150 m in length, with a mercury content of up to 0.86 percent. The Surkhnow occurrence is restricted to a fault zone, 100 to 400 m wide and over 2.0 km in strike length. Disseminated mercury mineralization has been found in three segments of heavily altered rocks that have a mercury content of up to 0.25 percent. Smaller mineralized zones with lower mercury content were described by Abdullah and others (1977) for Koh-e-Katif, Pasaband, Sebak, and Qasem.

The following seven mercury occurrences in the Sahebdad Khanjar subarea are described by Abdullah and others (1977). Khanjar covers over 1 km and had the highest values in mercury assays (0.35 to 0.96 percent). Qalat had the second highest mercury content of the occurrences (up to 0.44 percent). The other occurrences, Alibali, Alibali-I, Alibali-II, Gulgadam, and Sahebdad, have average mercury content of less than 0.1 percent.

The following 4 mineral occurrences (3 mercury and 1 copper) in the Pahjshah Mullayan subarea are described by Abdullah and others (1977). Generally, mercury concentrations in this subarea assayed at the lowest values of all the subareas. The Mullayan occurrence consists of two areas: a small area, 3.5 × 2.0 m in size, with mercury content 0.01 percent; and a larger area, up to 9 m in width and 200 m in length, which assayed at 0.09 percent mercury. The Panjshah occurrence is sparingly disseminated with mercury, having a content between 0.001 and 0.05 percent. An unnamed mineral showing, between 25 to 60 m long and 7 to 8 m thick, assayed at 0.005 percent mercury. The Gariba skarn copper occurrence is described as occurring in Early Cretaceous limestone in contact with Late Cretaceous-Paleocene diorite. The skarn zone is 3 km long, and 40 to 60 m thick, and assayed at 0.18 to 3.24 percent copper.

9B.4 Mineral Maps of the Kharnak-Kanjar Area of Interest

Analysis of the HyMap imaging spectrometer data of the Kharnak-Kanjar AOI using spectroscopic methods resulted in the identification of a wide variety of minerals exposed at the surface. Although the occurrence of certain minerals may suggest that mineralization processes may have once operated in the area, many of the minerals that were identified are also common rock-forming minerals or minerals that can be derived from the weathering of a wide variety of rock types. Consequently, knowledge about the distribution patterns of the identified minerals and the geologic context in which they occur is essential to understanding the causes of mapped mineral occurrences and evaluating the potential for related mineral deposits.

Figure 9B–6 depicts the results of the MICA analyses of the HyMap data for the Kharnak-Kanjar AOI for the 2-µm materials, including clays, carbonates, phyllosilicates, sulfates, altered minerals and other materials. The mineral present most frequently in the Kharnak-Kanjar AOI was carbonate, mainly in the calcite and calcite-abundant classes. In addition, significant areas were also found to contain calcite mixed with muscovite or clay classes. However, pixels with the best match to muscovite or illite spectra were identified over large contiguous areas in the southeastern and northwestern portions of the AOI. Distinct patterns of kaolinite clays also occur, especially in the east-central portion of the AOI.

Epidote and chlorite were present in spatially consistent patterns in the southeastern part of the AOI, along the southern boundary of the AOI, and near the western boundary of the AOI. Other classes with spatially contiguous patterns covering smaller areas include iron-bearing carbonate, alunite + kaolinite, pyrophyllite, and buddingtonite.

Figure 9B–7 shows the MICA 1-µm results for the iron-bearing minerals. Hematite was present in solid contiguous zones throughout the Kharnak-Kanjar AOI. The most abundant mineral in this map was goethite. The mixed "Fe^{2+} Fe^{3+} Type 1" class also covered a large fraction of the AOI and was concentrated in two areas, namely, the central portion of the southern boundary, and near the southeastern corner. Epidote was identified near the locations of pixels mapped as "Epidote or Chlorite" in the 2-µm map (fig. 9B–6).

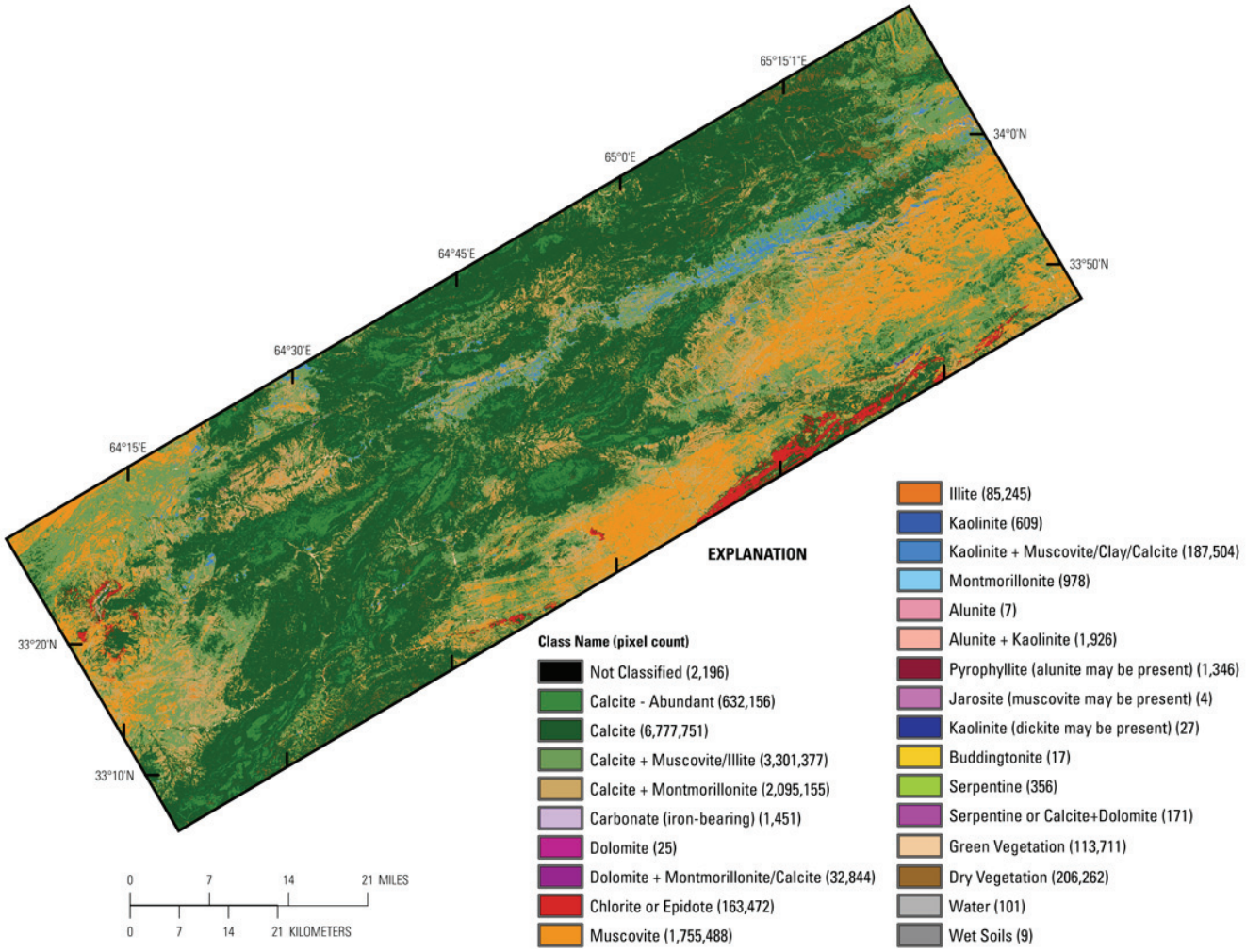

Figure 9B–6. Map showing carbonates, phyllosilicates, sulfates, altered minerals, and other materials derived from HyMap data in the Kharnak-Kanjar area of interest.

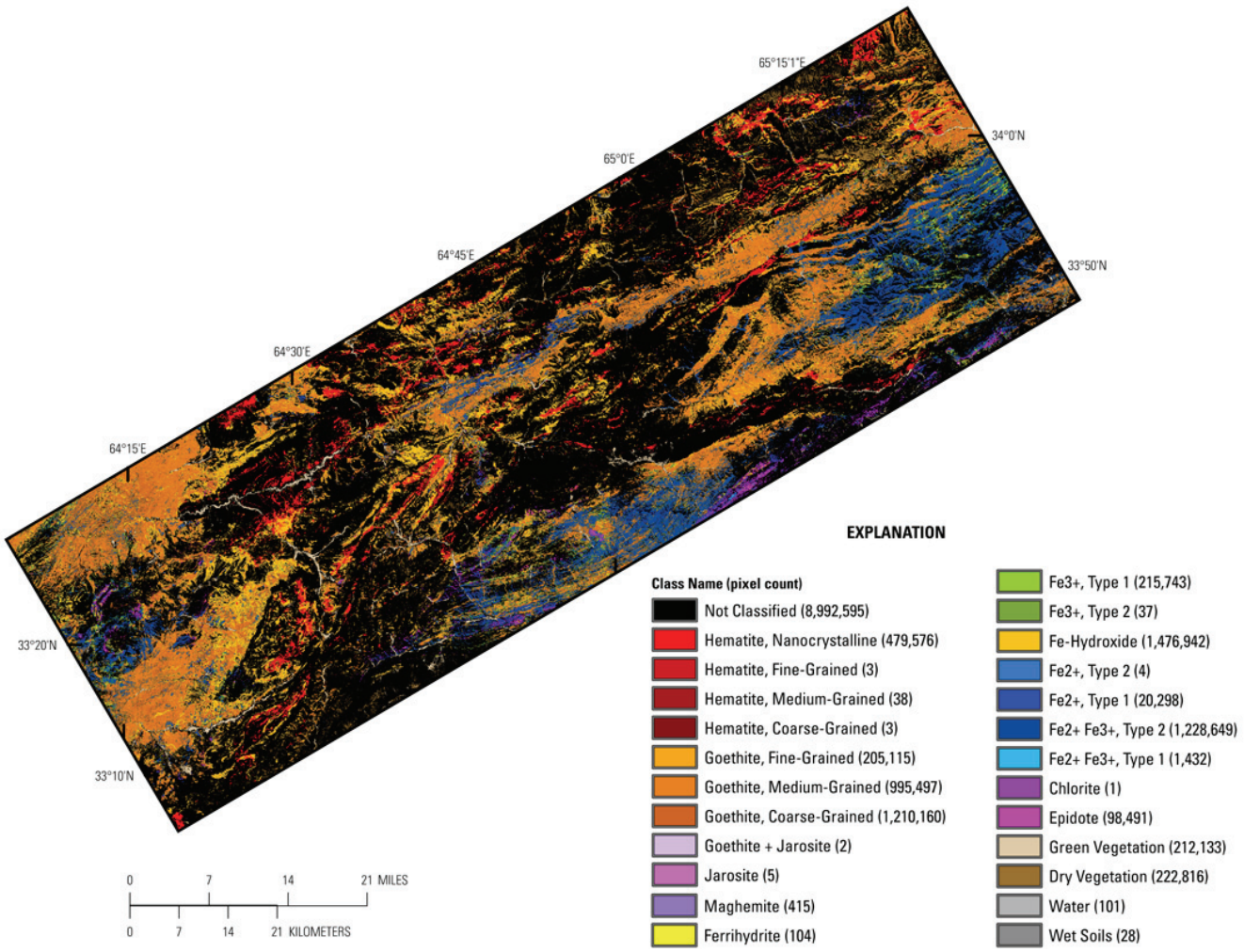

Figure 9B–7. Map showing iron-bearing minerals and other materials derived from HyMap data in the Kharnak-Kanjar area of interest.

Because of the large number of classes represented and the subtleties of the distribution patterns represented in these image maps, it is instructive to display these results as a series of image maps, each depicting a selected group of minerals that are mineralogically related or commonly occur together in specific geologic environments. The following sections first discuss these thematic maps of the full AOI, concentrating on the relationships between surface minerals and the mapped rock types, and then maps of surface minerals for the three subareas with discussion of the relationships between the imaging spectrometer results and the known mineral occurrences.

9B.4.1 Carbonate Minerals

A comparison of the geologic map (fig. 9B–4) with the carbonate minerals map shown with geologic contacts overlain (fig. 9B–8) reveals some relationships between the calcite classes and the Early Cretaceous stratified rock units of the Kharnak-Kanjar AOI. In general, mapped areas of the younger Early Cretaceous rocks in the Barremian-Aptian category are identified as matching the pure calcite spectra of the calcite and calcite-abundant classes. In contrast, polygons of the Berriasian-Valanginian category of Early Cretaceous rocks have very little of their area mapped in the pure calcite classes; most of the area of these polygons is matched to classes containing calcite mixed with montmorillonite or muscovite, or to classes that do not contain calcite. The Valanginian-Hauterivian category has intermediate composition; polygons of this unit contain some pixels with strong calcite

absorption features, but more often, the spectra of pixels in this category are matched to kaolinite mixed with calcite (in the eastern part of the AOI) or to calcite mixed with muscovite or clay (in the western part of the AOI). Iron-bearing carbonate was detected primarily in and around the larger polygon of intrusive Oligocene rocks at the western boundary of the AOI.

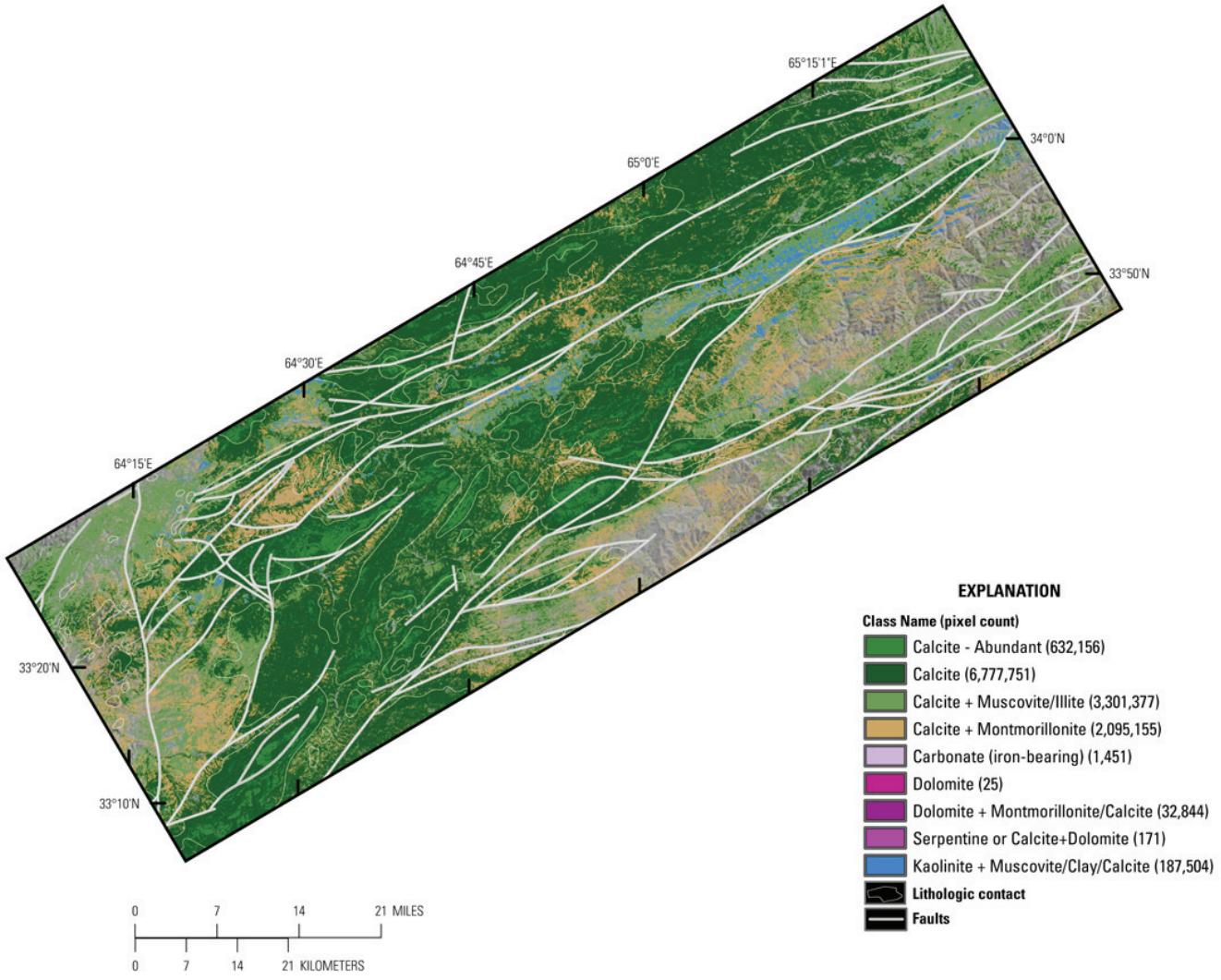

Figure 9B–8. Map showing distribution of carbonate minerals derived from HyMap data in the Kharnak-Kanjar area of interest.

9B.4.2 Clays and Micas

The long unit of Valanginian-Hauterivian Early Cretaceous rocks containing kaolinite mixed with calcite (in the eastern part of the AOI) is highlighted well in the clays and micas map (fig. 9B–9). Most pixels matching reference entries containing kaolinite are within this category of the geologic map. The "chlorite or epidote" class is strongly associated with the Late Jurassic/Early Cretaceous stratified and intrusive rock units at the southern boundary of the eastern part of the Kharnak-Kanjar AOI. This class is also associated with the Oligocene intrusive rock unit at the western boundary of the AOI. Polygons of the Berriasian-Valanginian category of Early Cretaceous rocks, which had little of their area mapped in the pure calcite classes (see fig. 9B–8), have most of their area matched to muscovite and illite classes (fig. 9B–9). Because these classes cover a large portion of the AOI, more detailed discriminations are made in a separate map of muscovites and illite (fig. 9B–10). Most of the micas fall into the medium-high-aluminum-content class of muscovite. However, there are significant stratified

patterns of low and medium-high-aluminum-content muscovites in the Berriasian-Valanginian unit in the eastern part of the AOI.

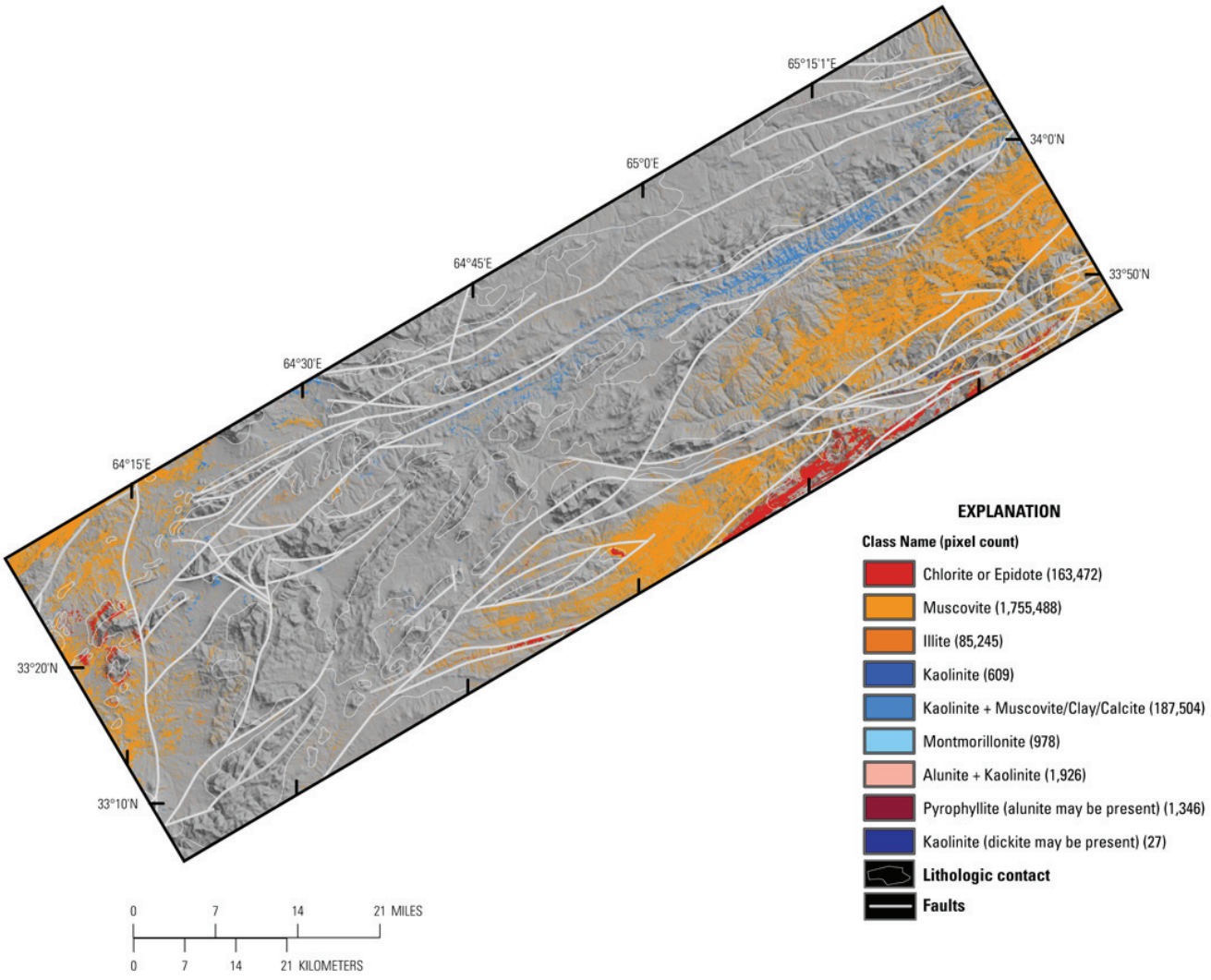

Figure 9B–9. Map showing distribution of clay and mica minerals derived from HyMap data in the Kharnak-Kanjar area of interest.

9B.4.3 Iron Oxides and Hydroxides

Hematite was present in contiguous zones throughout the Kharnak-Kanjar AOI (fig. 9B–11). The most abundant mineral in this map was goethite. The iron-oxides and hydroxides are present throughout the AOI and are not associated with any particular rock type. The Eocene-Oligocene stratified rock units in the southern part of the AOI are distinct in the near-complete absence of iron oxides and hydroxides within their boundaries.

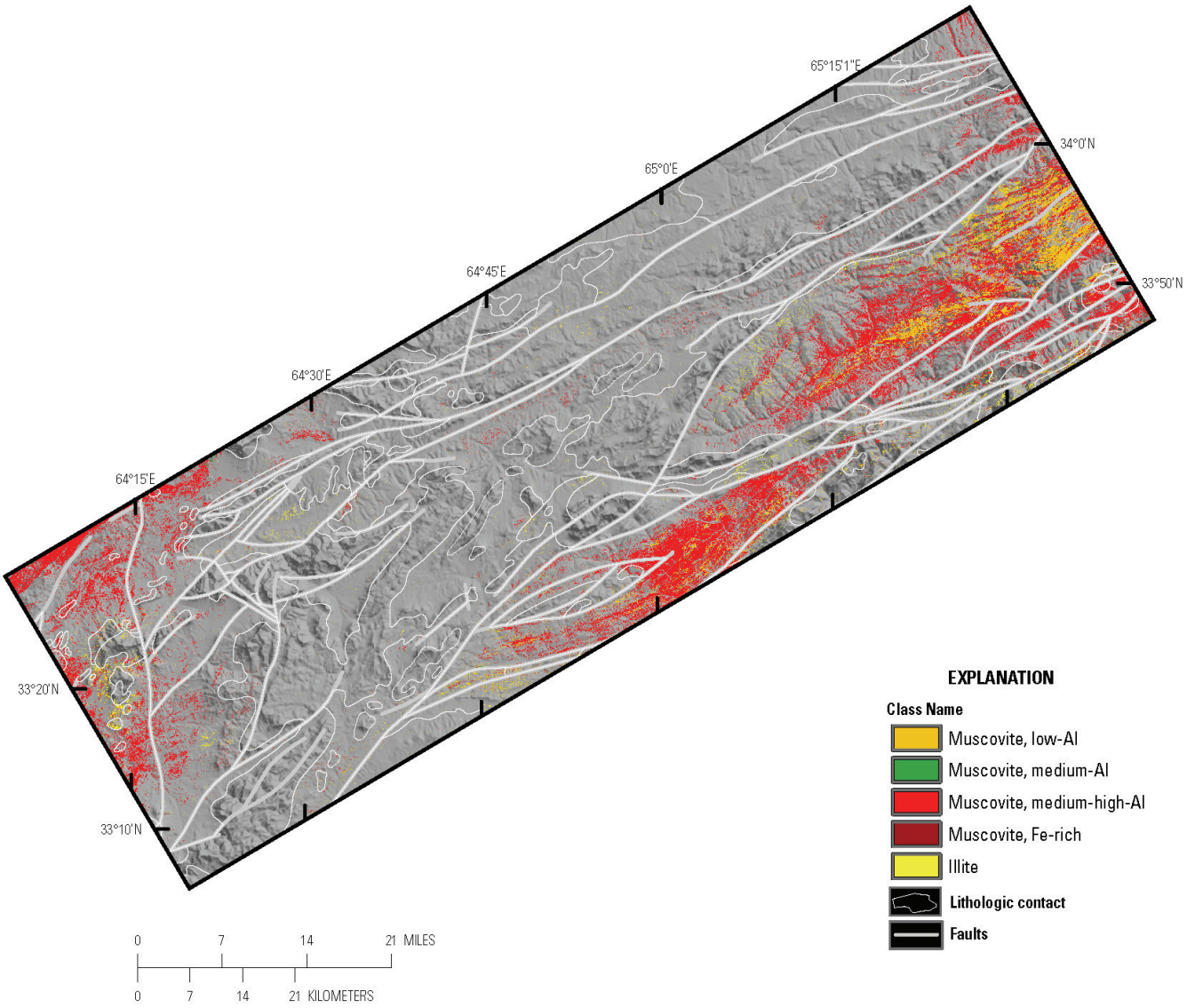

Figure 9B–10. Map showing muscovites and illites derived from HyMap data in the Kharnak-Kanjar area of interest.

9B.4.4 Common Alteration Minerals

Most of the minerals in this group are commonly present in hydrothermally altered rocks associated with epithermal mineral deposits (fig. 9B–12). Consequently, clustered occurrences are of great interest in terms of potential mineral deposits. In some areas, the mineral distributions are suggestive of hydrothermal alteration in the Kharnak-Kanjar AOI; the most extensive of these are delineated on figure 9B–12. Kaolinite mixed with calcite in the long unit of Valanginian-Hauterivian Early Cretaceous rocks, described previously, also contains concentrations of pixels matched to the kaolinite and kaolinite mixed with alunite classes. Other similar patterns occur in the Early Cretaceous rocks in the Kharnak-Kanjar AOI; these areas are circled with a green dashed line. Kaolinite containing possible dickite is also present within these zones. Visual inspection of the spectra confirmed there are variations in the kaolinite clay absorption in these areas, but spectra with strong absorption features indicative of abundant dickite or alunite concentrated within pixels were not found in this preliminary analysis. Mineral mixtures of kaolinite with small amounts of dickite and/or alunite are more consistent

with the spectra of these pixels. Additional studies of the spectra in these areas should be conducted in conjunction with laboratory spectroscopy and other mineral assays of samples from these areas.

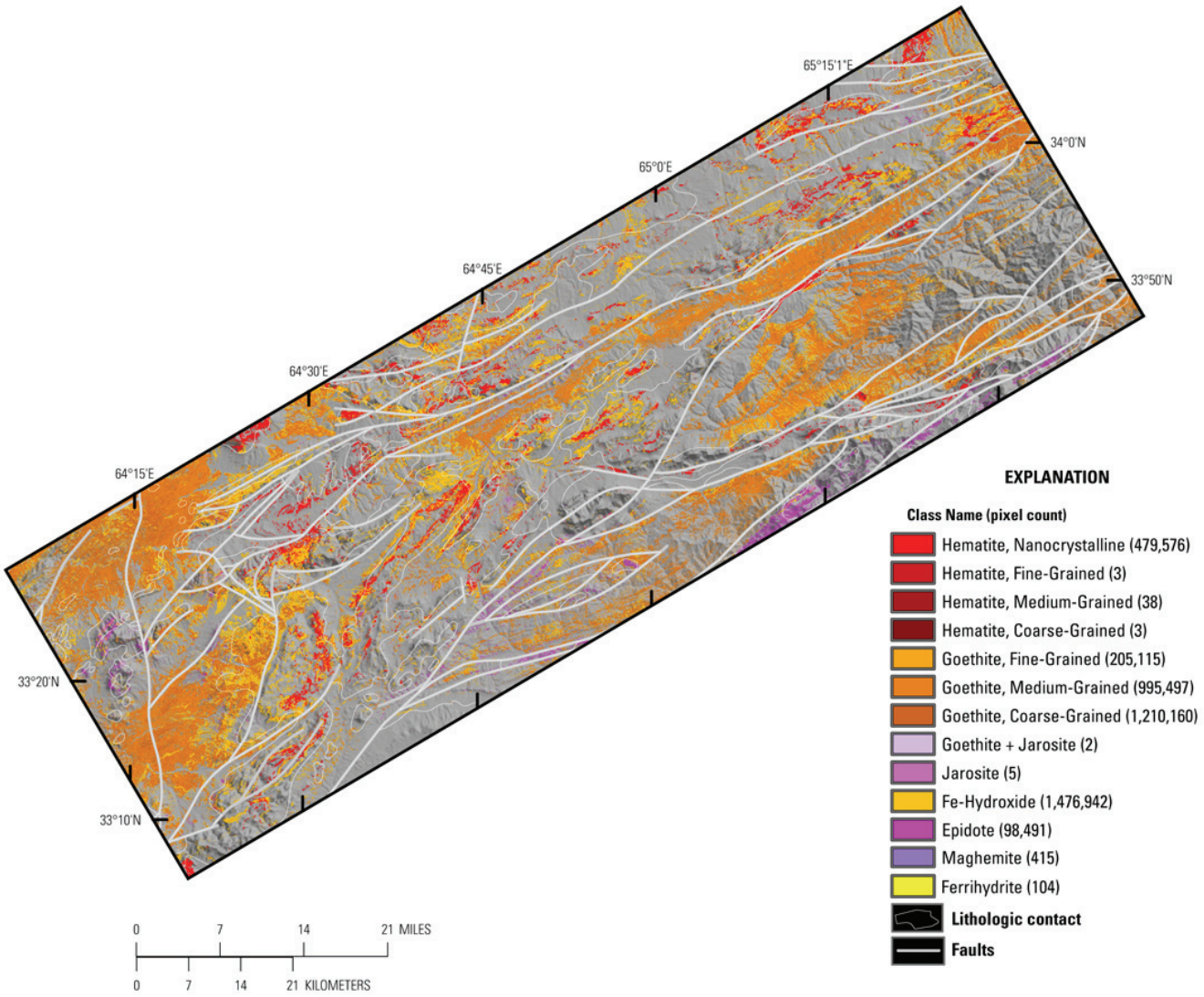

Figure 9B–11. Map showing distribution of iron oxide and hydroxide derived from HyMap data in the Kharnak-Kanjar area of interest.

Only 17 pixels matching the spectrum of buddingtonite, an ammonium bearing feldspar formed hydrothermally and a possible indicator of gold and silver deposits, were detected. The spectra are strongly indicative of the mineral, however, and occur in a spatially contiguous pattern near areas matched to spectra of kaolinite and kaolinite mixed with alunite (shown within the orange rectangle in figure 9B–12. Pixels adjacent to the detected occurrences of buddingtonite also exhibit an absorption feature at the 2.11-µm wavelength position, consistent with buddingtonite's primary absorption feature in HyMap data, in addition to an absorption feature at 2.2 µm from mica or clay. Therefore, a subsequent MICA analysis of the imaging spectrometer data in the area was conducted, adding a spectrum of buddingtonite and montmorillonite to the reference library. The results of the new analysis (fig. 9B–13) confirmed the presence of buddingtonite in more pixels than the original analysis (95 pixels, equivalent to an area of 5 hectares). The buddingtonite detected in the imaging spectrometer data is mostly within the mapped unit of Valanginian-Hauterivian Early Cretaceous rocks, with the kaolinite and alunite detected along the contact with Pliocene rocks nearby (fig. 9B–12). None of the known mercury occurrences in the Kharnak-Kanjar AOI are located in the vicinity of the buddingtonite area. Because buddingtonite can be indicative of hydrothermal alteration associated with mercury deposits, additional

study of this area is recommended, including detailed geological mapping, lithologic sampling, and geochemical studies.

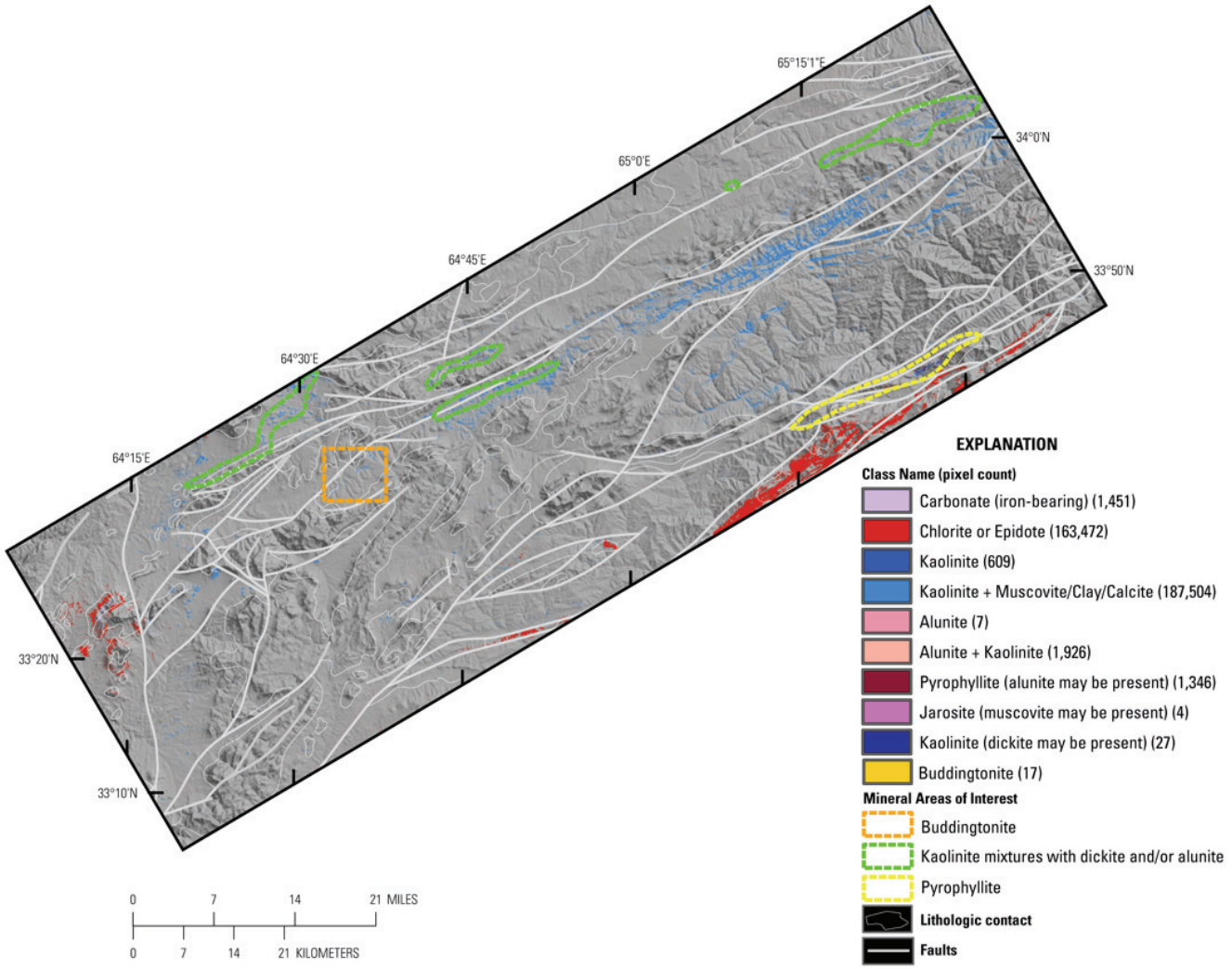

Figure 9B–12. Map showing distribution of common alteration minerals derived from HyMap data in the Kharnak-Kanjar area of interest.

An extensive area of pixels was present that matches the spectrum of pyrophyllite, a phyllosilicate that can be formed hydrothermally and is a possible indicator of gold and silver deposits. The spectra are strongly indicative of the mineral and occur in a spatially contiguous pattern surrounded by pixels matched to spectra of kaolinite and kaolinite mixed with alunite (shown within the yellow circle in figure 9B–12). Pixels adjacent to the detected occurrences of pyrophyllite also exhibit a narrow absorption feature at the 2.168-µm wavelength position, consistent with pyrophyllite's primary absorption feature in HyMap data. An enlargement of this area is shown in fig. 9B–14, along with a perspective view of the pixels matched to pyrophyllite, kaolinite, and alunite minerals. This map was derived from the revised analysis of the Kharnak-Kanjar AOI (see previous discussion of buddingtonite). The main pyrophyllite zone is over 13 km long and up to 7 km wide. A second area of scattered pixels matched to pyrophyllite occurs to the southwest of the main zone, and is over 2.5 km long and up to 1.5 km wide. The pyrophyllite, kaolinite, and alunite detected in the imaging spectrometer data are within the mapped unit of Valanginian-Hauterivian Early Cretaceous rocks (fig. 9B–12). The spectra of pixels in this area have the strongest alunite absorption features of any pixels matched to this mineral in the Kharnak-Kanjar AOI. None of the known mercury occurrences in Kharnak-Kanjar AOI are located in the vicinity of the pyrophyllite area. Because pyrophyllite can be

indicative of hydrothermal alteration associated with metallic ore deposits, additional detailed study of this area relating the spectral identifications to geologic mapping is recommended to determine whether field surveys for lithologic and geochemical sampling are warranted.

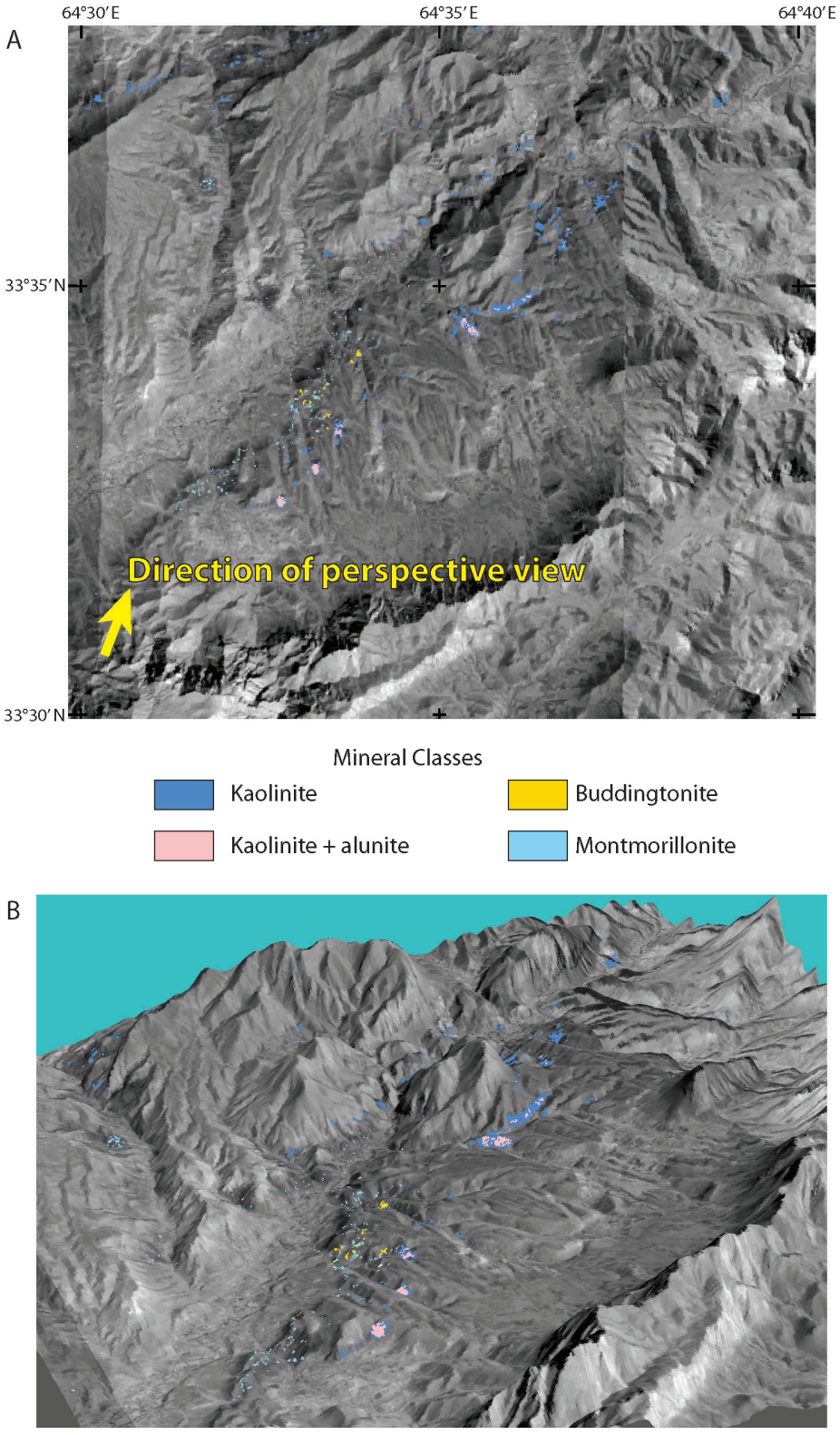

Figure 9B–13. (*A*) Detailed map of buddingtonite and other alteration minerals derived from HyMap data for a selected portion of the Kharnak-Kanjar area of interest. (*B*) 3D view of the detailed area looking north-northeast.

9B.4.5 Common Secondary Minerals

Epidote and chlorite were present in spatially consistent patterns in the southeastern part of the AOI, as well as along its southern and western boundaries (fig. 9B–15). Along the southern boundary of the AOI, both minerals are present in the polygons of Late Jurassic-Early Cretaceous rocks. In the western part of the AOI, these minerals are detected within and adjacent to the mapped polygon of intrusive rocks of Oligocene age. In some cases, the epidote class, as shown on the 1-μm map (fig. 9B–11), may be confused with calcite. Serpentine classes were detected in a scattered pattern in two areas of the AOI. Inspection of the spectra of these pixels revealed weak features at 2.3 μm, and sometimes at 2.2 μm, with relatively low reflectance levels. The pixels with low reflectance had low signal-to-noise ratio (S/N) and noisy absorption features, which likely resulted in misidentification of these pixels as serpentine, as evidenced by the relatively low fit values. The fit value is the comparison value used by the MICA analysis to compare pixel spectra to reference spectra (Kokaly, 2011). In addition, the low S/N may have led to misidentification in pixels adjacent to the serpentine detections. A false-color composite of three HyMap bands (red, green and blue loaded with HyMap channels 111, 86, and 6, equivalent to 2.272, 1.738, and 0.542 μm, respectively) highlights these rocks with purple and blue shading (figure 9B–16). It is possible that the spectral library does not have a representative entry for the mineral or mineral mixture of rocks in these areas. In general, the reflectance spectra in these pixels bear close resemblance to the spectra of unidentified rocks found in the Panjsher Valley AOI (fig. 13B–7 of chap. 13B in this report).

9B.4.6 Koh-e-Katif Passaband Subarea

A contrast-enhanced stretch of the natural color composite of Landsat Thematic Mapper bands in figure 9B–17 provides a general overview of the Koh-e-Katif Passaband subarea of the Kharnak-Kanjar AOI terrain, and is useful for understanding the general characteristics and distribution of surficial material, including rocks and soil, unconsolidated sediments, vegetation, and hydrologic features. Figure 9B–18 shows the geologic setting of the nine mercury occurrences in the Koh-e-Katif Passaband subarea, including Kharnak, Koh-e-Katif, Pasaband, Pushwara, Sebak, Qasem, Surkhnow, Katif, and Duwalak.

Kaolinite mixed with calcite and kaolinite classes were mapped in the vicinity of the Kharnak and Pushwara occurrences (fig. 9B–19). The pixels matched to kaolinite are over 1 km in length with a width of approximately 200 m around the Kharnak occurrence and have spectra with a strong 2.2-μm doublet absorption feature of kaolinite. A line of scattered kaolinite mixed with calcite pixels trends 2 km to the southwest from the mapped location of the Pushwara occurrence. The patterns of kaolinite near both these occurrences roughly correspond to their descriptions in Abdullah and others (1977). The spectral features in the imaging spectrometer data of the pixels matched to kaolinite strongly contrast with the surrounding pixels matched to calcite (which have a strong carbonate absorption feature at 2.3 μm and, at most, a very weak clay absorption feature at 2.2 μm), indicating localized enrichment of kaolinite. The intermediate spectra between these two types of rocks were matched to calcite mixed with clay (montmorillonite or illite) or muscovite, in which a 2.3-μm feature is present and the 2.2-μm feature is weakened and appears, at times, more like a singlet absorption. Dickite has an absorption feature at the same 2.2-μm position as kaolinite with a slightly different shape. It is possible that variations in the 2.2-μm feature may be indicative of degree of dickitization; however, this relationship should be clarified from additional lithologic sampling, as well as field and laboratory spectroscopy and analyses.

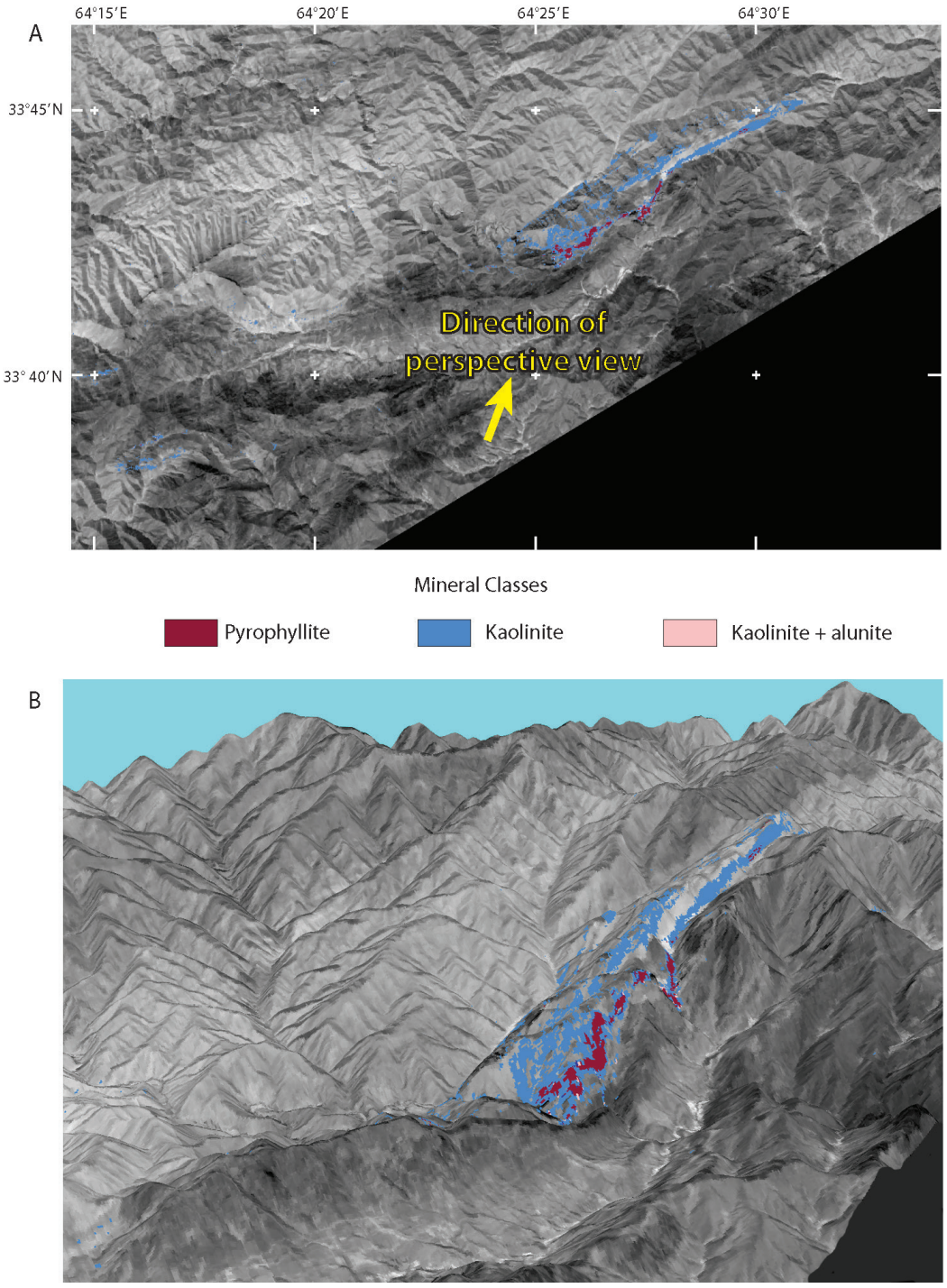

Figure 9B–14. (*A*) detailed map of pyrophyllite and other alteration minerals derived from HyMap data for a selected portion of the Kharnak-Kanjar area of interest. (*B*) 3D view of the detailed area looking to the north-northeast.

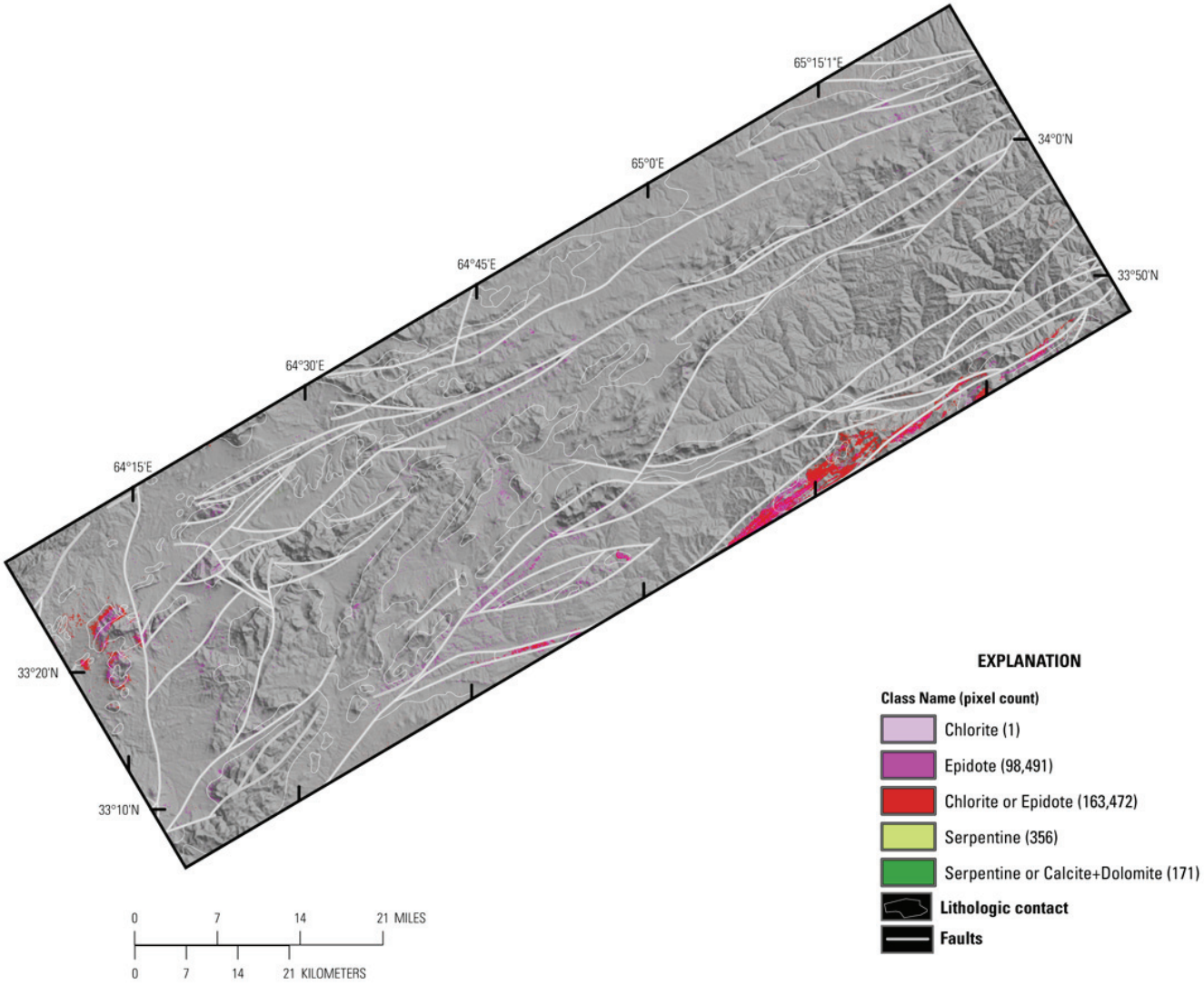

Figure 9B–15. Map showing distribution of common secondary minerals derived from HyMap data in the Kharnak-Kanjar area of interest.

The dominant iron-bearing minerals detected around the Kharnak and Pushwara mercury occurrences are goethite (fine-grained to coarse-grained) and iron-hydroxide (fig. 9B–20). Abdullah and others (1977) describe the Kharnak occurrence as having a stock consisting mainly of calcareous-dickitized metasomatites having variable iron-hydroxide content. The minerals detected in the HyMap imaging spectrometer agree closely with that description, specifically, patterns of kaolinite mixed with calcite and calcite mixed with clay/muscovite (in the 2-µm analysis), within areas mapped as containing goethite in the 1-µm analysis. Abdullah and others (1977) report that cinnabar was found in the area of the Pushwara occurrence. Cinnabar was not part of the reference spectral library used in this preliminary analysis of the HyMap imaging spectrometer data. Refinement of the MICA analysis to detect cinnabar using spectra of rock samples from the occurrences is recommended for future studies.

Similar to the results around the Kharnak mineral occurrence, patterns of kaolinite mixed with calcite and calcite mixed with clay/muscovite, within areas mapped as containing goethite, are found within 300 m of the Duwalak and Surkhnow mineral occurrences. The mineral patterns are confined to smaller areas than those present around the Kharnak and Pushwara occurrences. With the exception of these four sites, the other mercury occurrences were present in areas matched to calcite mixed with clay/muscovite, with spectra that resemble mixtures of calcite and kaolinite. However, areas in the vicinity of these mineral occurrences have a mineral pattern very similar to the Kharnak and Pushwara

mineral occurrences. Two kilometers southeast of the indicated locations of the Qasem, Koh-i-Katif, Katif, and Duwalak occurrences is an area having this pattern, including kaolinite with possible alunite (lat 33°26'04" N., long 64°39'37" E.). A few more kilometers to the southeast of that area is an even larger area with this pattern (lat 33°23'29" N., long 64°38'10" E.). Near the northwest corner of the Kohe-Katif Passaband subarea of the Kharnak-Kanjar AOI, is the area described earlier (lat 33°33'39" N., long 64°33'06" E.) as containing buddingtonite, kaolinite and alunite, indicating potential hydrothermal alteration (fig. 9B–19, northwest corner; fig. 9B–13*A*). These three locations should be included as potential field sampling sites in future studies of the subarea.

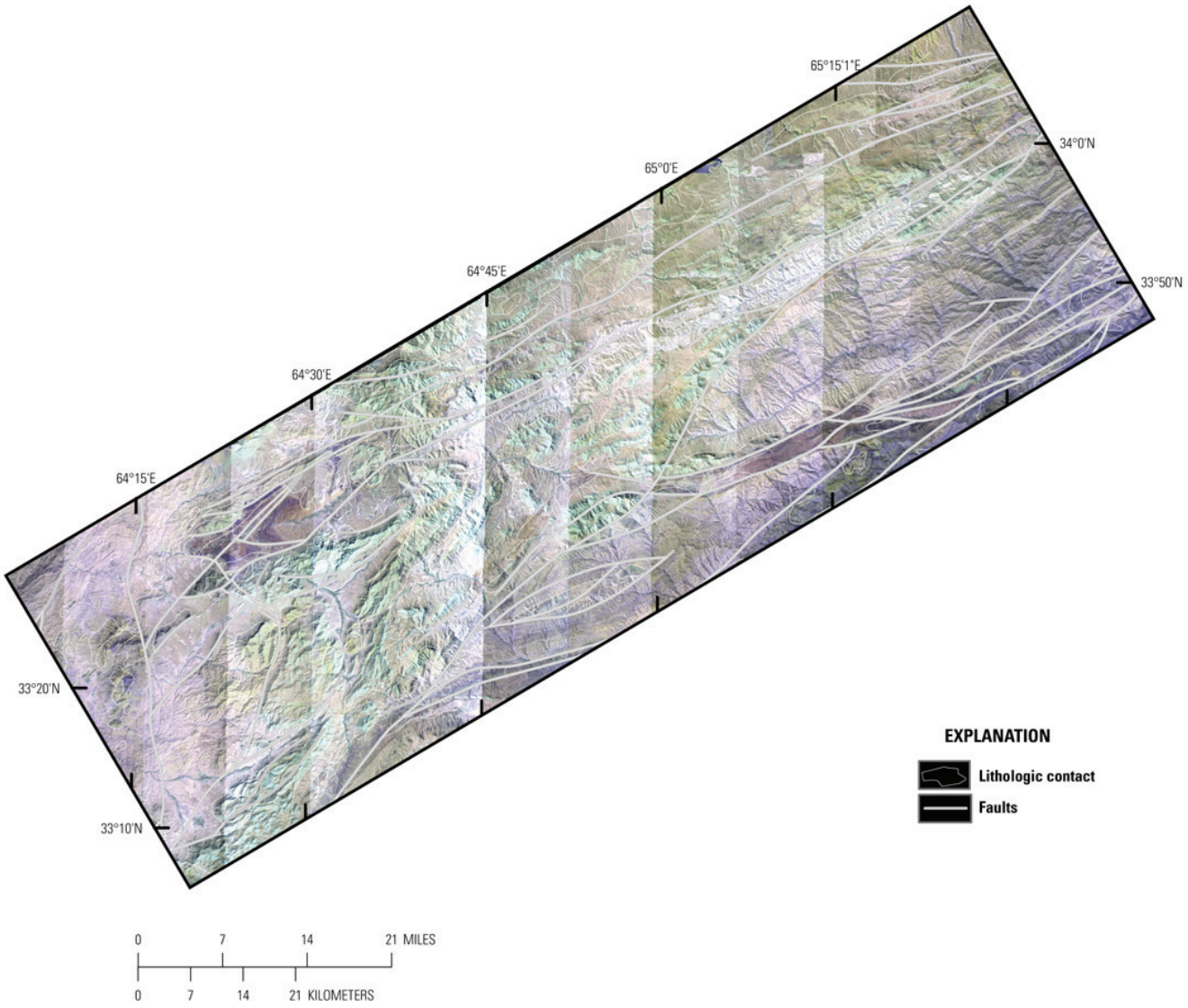

Figure 9B–16. False-color composite derived from HyMap data in the Kharnak-Kanjar area of interest. Channels at 2.27, 1.73, and 0.54 micrometers were loaded into the red, green, and blue colors, respectively.

9B.4.7 Sahebdad Khanjar Subarea

A contrast-enhanced stretch of the natural-color composite of Landsat Thematic Mapper bands in figure 9B–21 provides a general overview of the Sahebdad Khanjar subarea of the Kharnak-Kanjar AOI terrain, and is useful for understanding the general characteristics and distribution of surficial material, including rocks and soil, unconsolidated sediments, vegetation, and hydrologic features. Figure 9B–22 shows the geologic setting of the seven mercury occurrences in the Sahebdad Khanjar subarea, including Khanjar, Qalat, Alibali, Alibali-I, Alibali-II, Gulgadam, and Sahebdad.

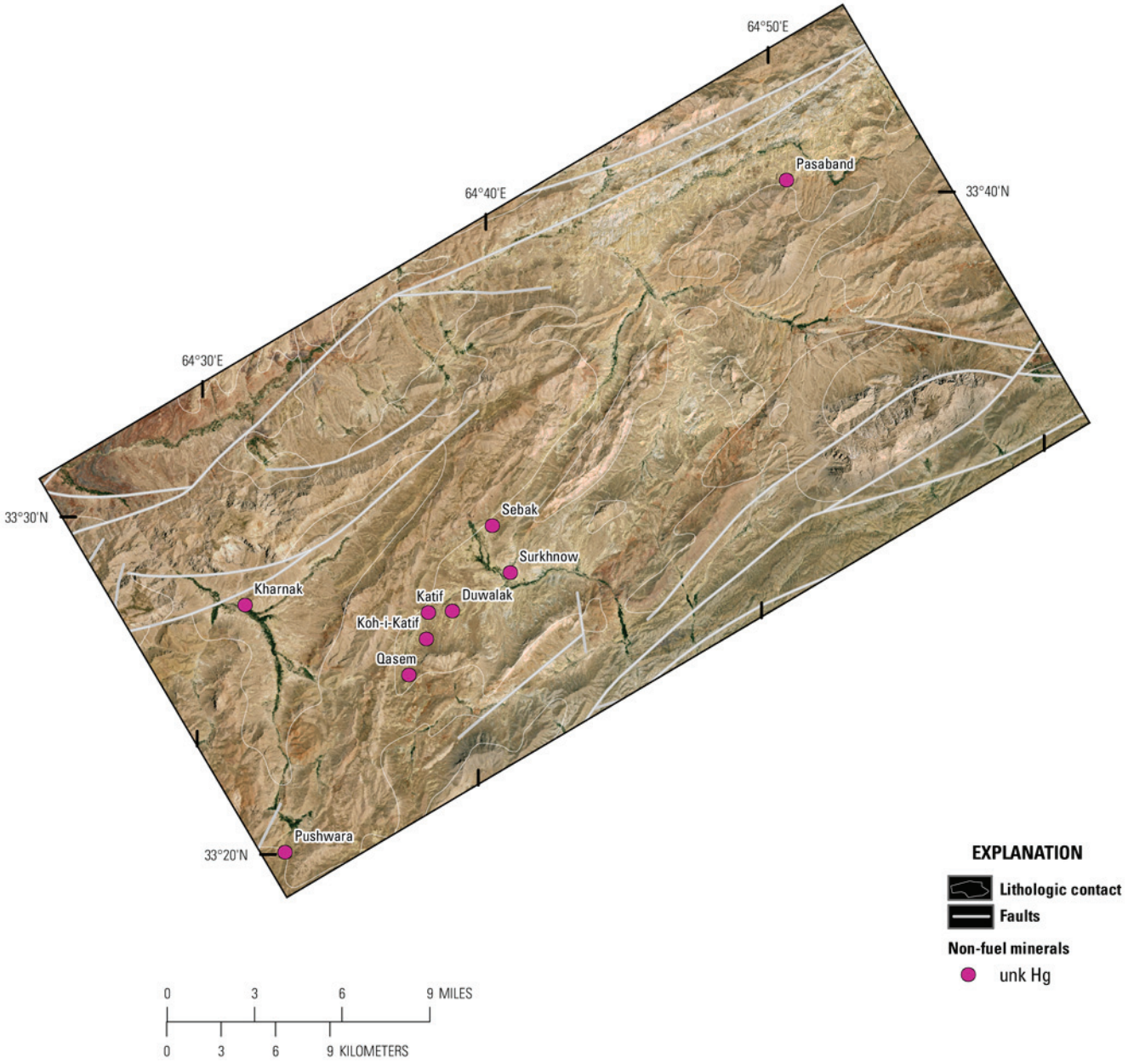

Figure 9B–17. Contrast-enhanced Landsat Thematic Mapper natural color image of the Koh-e-Katif Passaband subarea of the Kharnak-Kanjar area of interest. Geologic units and faults from Abdullah and Chmyriov (1977). unk, unknown.

Minerals detected around the mercury occurrences in the Sahebdad Khanjar subarea are similar to those found in the Koh-e-Katif Passaband subarea; pixels matched to kaolinite and kaolinite mixed with other minerals, within a more widespread detection of calcite plus muscovite or clay in the 2-µm map and goethite in the 1-µm map (figs. 9B–23 and 9B–24, respectively). However, more spectra matched to muscovite and kaolinite mixed with muscovite in Sahebdad Khanjar. The mineral occurrences are within or near pixels that were matched best to kaolinite or kaolinite mixed with calcite or muscovite.

As in the Koh-e-Katif Passaband subarea, the Sahebdad Khanjar subarea has several areas with mineral patterns similar to those near mercury occurrences located far from known mineral occurrences. Specifically, in the 2-µm map (fig. 9B–23), these areas contain pixels matched to kaolinite with a strong absorption feature, and pixels matched to kaolinite with possible alunite; in the 1-µm map (fig. 9B–24), pixels are matched to goethite (dominantly coarse-grained goethite). The three largest of these areas,

each greater than 16 hectares, are noted here, including an area in the northwestern corner of the subarea at lat 34°02'11"N., long 65°29'39" E., an area near the middle of the subarea at lat 33°58'13" N., 65°17'24" E., and one closer to the southern boundary of the subarea at lat 33°47'45" N, long 65°00'45" E. In future studies of the Sahebdad Khanjar subarea, these three locations should be included as potential field sampling sites.

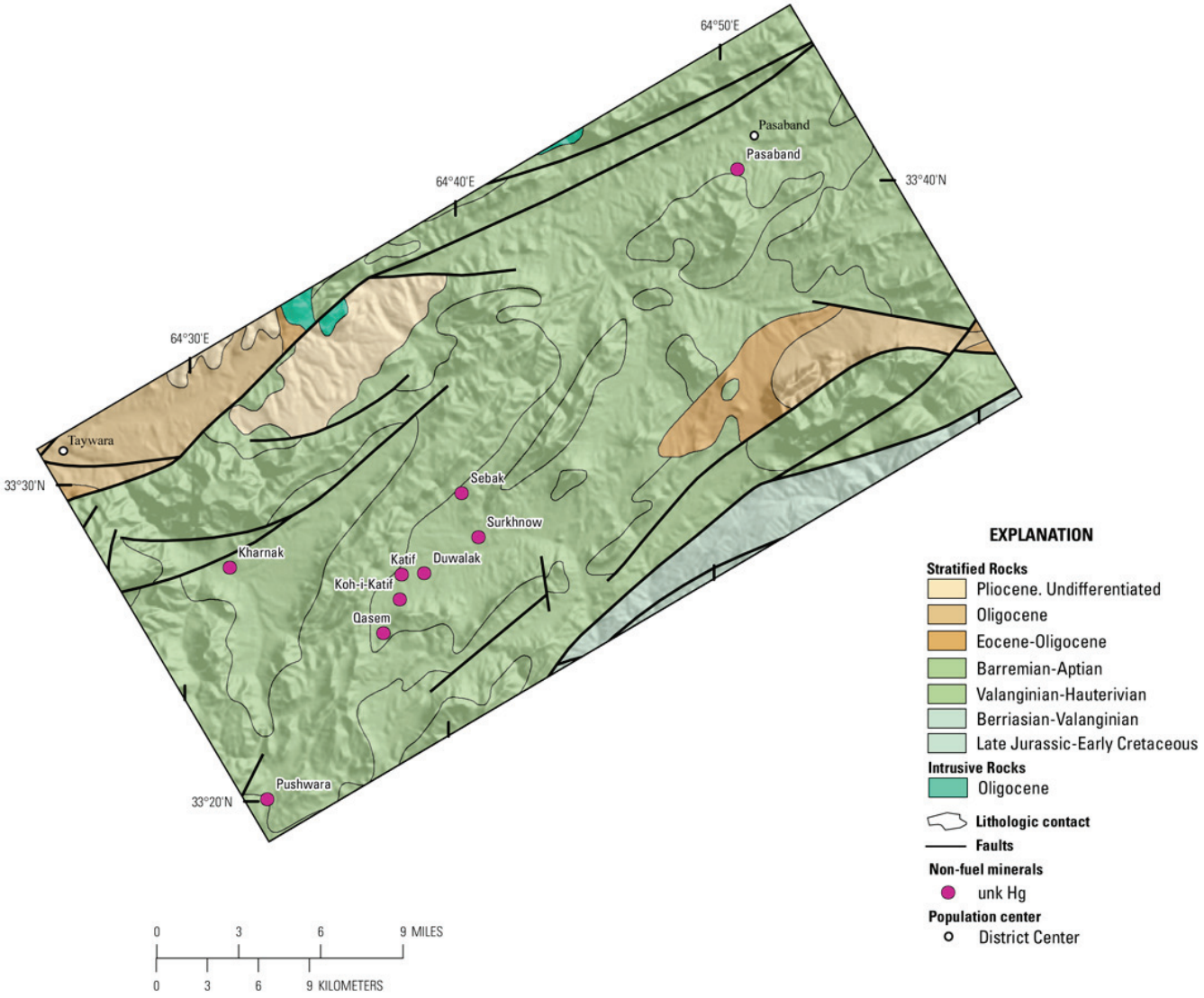

Figure 9B–18. Map showing sites of mercury mineralization (Peters and others, 2007) in relation to local geology of the Koh-e-Katif Passaband subarea of the Kharnak-Kanjar area of interest. Geology from digital geologic map of Afghanistan (Abdullah and Chmyriov, 1977; Doebrich and Wahl, 2006; Peters and others, 2007). unk, unknown.

9B.4.7 Pahjshah Mullayan Subarea

A contrast-enhanced stretch of the natural color composite of Landsat Thematic Mapper bands in figure 9B–25 provides a general overview of the Pahjshah Mullayan subarea of the Kharnak-Kanjar AOI terrain, and is useful for understanding the general characteristics and distribution of surficial material, including rocks and soil, unconsolidated sediments, vegetation, and hydrologic features. Figure 9B–26 shows the geologic setting of the four mineral occurrences in the Pahjshah Mullayan subarea, including three mercury occurrences, Mullayan, Panjshah, and an unnamed site; and one skarn copper occurrence, Gariba.

Minerals detected around the Mullayan occurrences in the Pahjshah Mullayan subarea are similar to those observed in the Koh-e-Katif Passaband subarea; small areas of kaolinite and kaolinite mixed with other minerals, within a more widespread detection of calcite plus muscovite or clay in the 2-µm analysis and goethite in the 1-µm analysis (figs. 9B–27 and 9B–28). This mineral occurrence is in pixels that were matched best to calcite mixed with clay/muscovite. The other mercury occurrences in this subarea are areas in which the pixels were matched to calcite. Kaolinite is more than 700 m from the unnamed occurrence, and more than 1 km from the Panjshah occurrence.

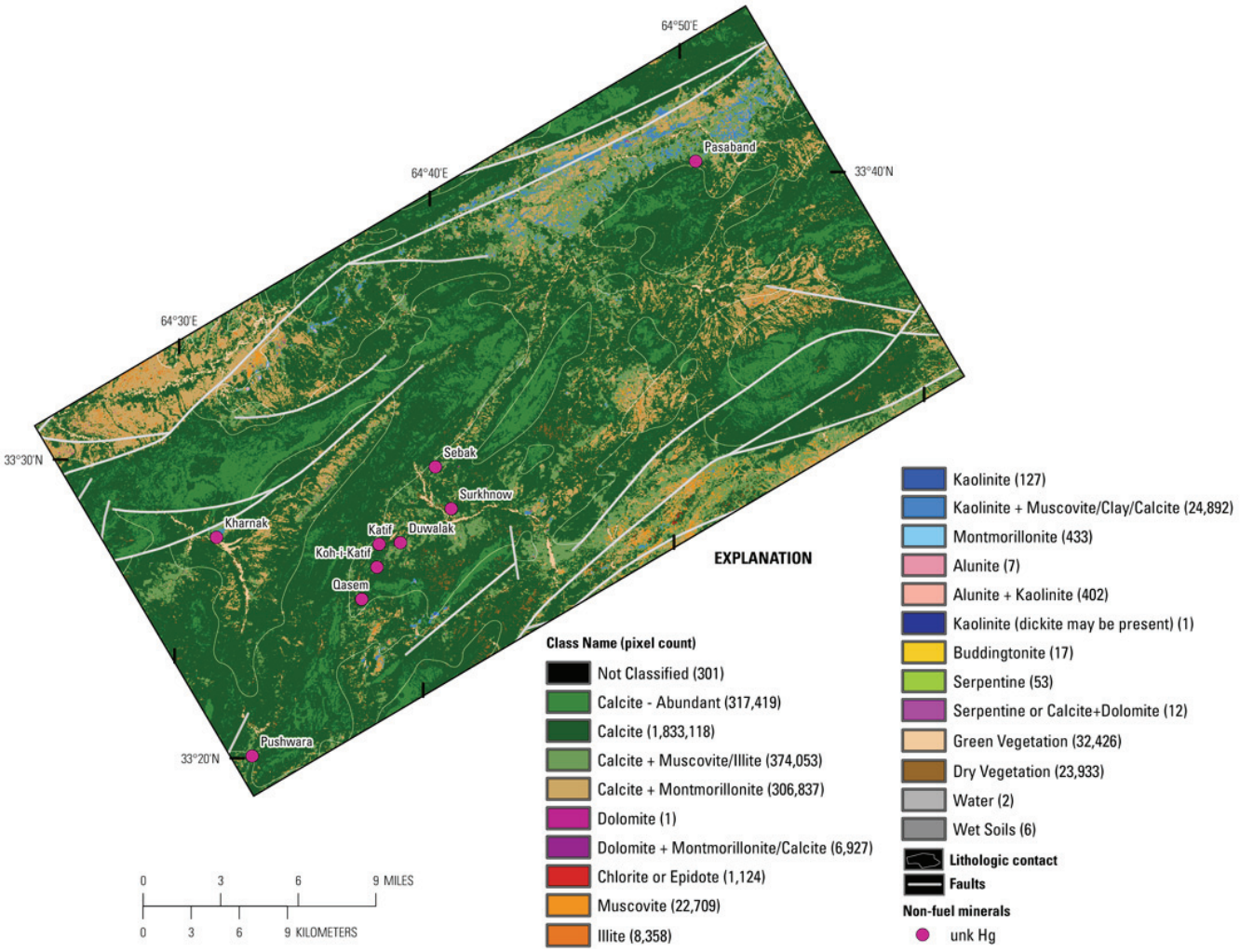

Figure 9B–19. Map showing carbonates, phyllosilicates, sulfates, altered minerals, and other materials derived from HyMap data in the Koh-e-Katif Passaband subarea of the Kharnak-Kanjar area of interest. unk, unknown.

As in the Koh-e-Katif Passaband subarea, the Sahebdad Khanjar subarea contains several areas with mineral patterns similar to those near mercury occurrences located far from known mineral occurrences. Specifically, in the 2-µm map (fig. 9B–27), these areas contain pixels matched to kaolinite with a strong absorption feature, and pixels matched to kaolinite with possible alunite; in the 1-µm map (fig. 9B–28), pixels are matched to goethite (primarily coarse-grained goethite). The three largest of these areas (each greater than 16 hectares) are noted here, including an area between the unnamed and the Mullayan mercury occurrences at lat 33°25'17" N, long 64°21'05" E, an area southeast of the Mullayan mercury occurrence at lat 33°25'11" N, long 64°25' 09" E., and one northeast of the Panjshah mercury occurrence at lat 33°31'24" N, long 64°21'20" E. Three pixels with strong buddingtonite absorption features, indicating potential hydrothermal alteration, were detected in the western boundary of the subarea at lat 33°21'44" N, long 64°12'42" E. In future studies of the Sahebdad Khanjar subarea, these locations should be included as potential field sampling sites.

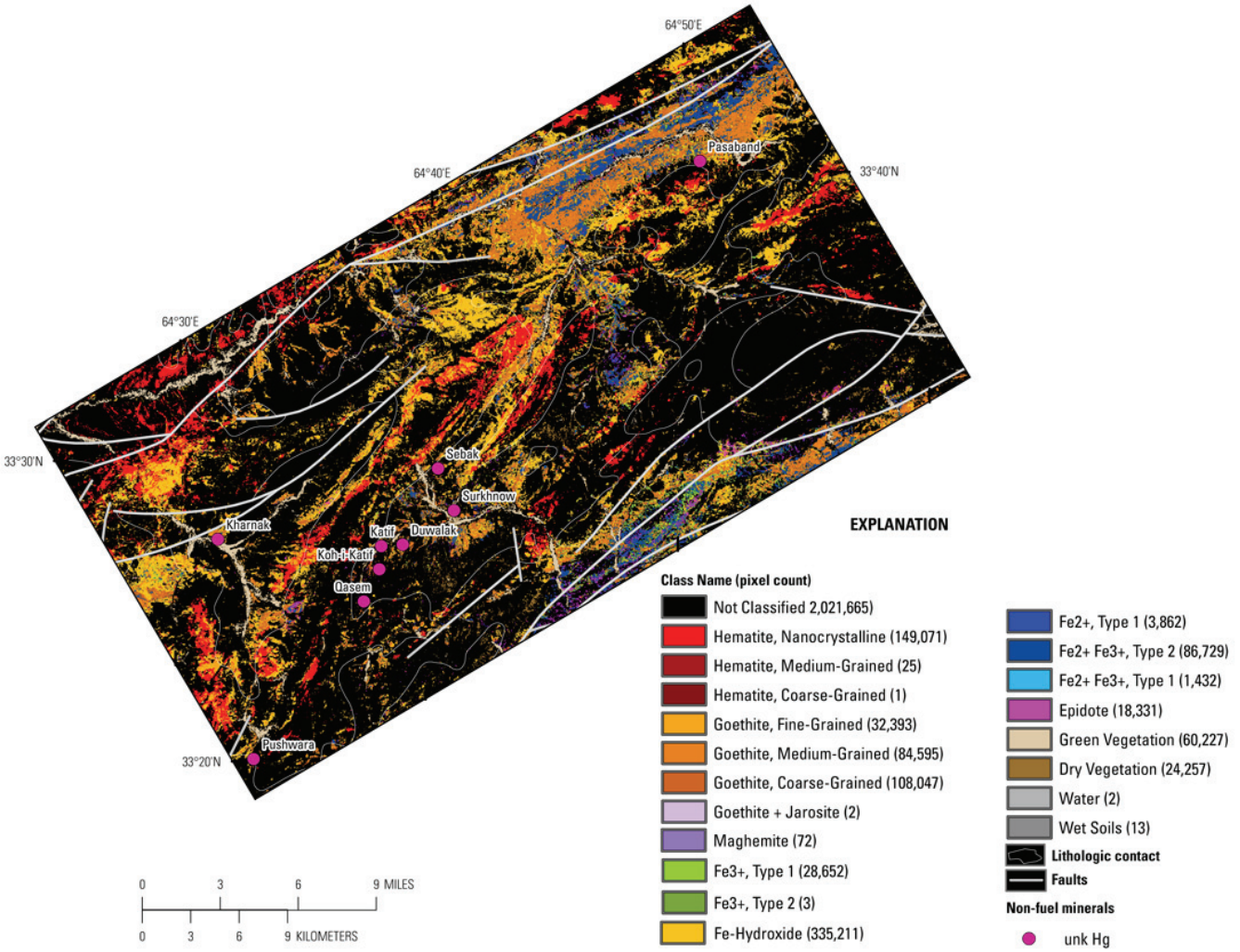

Figure 9B–20. Map showing iron-bearing minerals and other materials derived from HyMap data in the Koh-e-Katif Passaband subarea of the Kharnak-Kanjar area of interest. unk, unknown.

9B.5 Summary

The mineral class found most frequently in the Kharnak-Kanjar AOI was carbonate, mainly in the calcite and calcite–abundant classes. Significant areas were also found to contain calcite mixed with muscovite or clay classes. However, pixels with the best match to muscovite or illite spectra were also identified over large contiguous areas in the southeastern and northwestern portions of the AOI. Distinct patterns of kaolinite clays were detected, especially in the east-central portion of the AOI, concentrated within smaller areas. Epidote and chlorite were present in spatially consistent patterns in the southeastern part of the AOI, along the southern boundary of the AOI, and in and around the intrusive rocks near the western boundary of the AOI.

In general, pixels in polygons of the younger Early Cretaceous rocks in the Barremian-Aptian category were identified as matching the pure calcite spectra of the calcite and calcite-abundant classes. In contrast, polygons of the Berriasian-Valanginian category of Early Cretaceous rocks had very little of their area mapped in the pure calcite classes; most of the area of these polygons was matched to classes containing muscovite or illite. The Valanginian-Hauterivian category had intermediate composition, polygons of this unit contained some pixels with strong calcite absorption features, but more often the spectra of pixels in this category were matched to kaolinite mixed with calcite (in the eastern part of the AOI) or to calcite mixed with muscovite or clay (in the western part of the AOI).

Kaolinite mixed with calcite was detected primarily in the long unit of Valanginian-Hauterivian Early Cretaceous rocks, along with concentrations of pixels matched to the kaolinite and kaolinite mixed with alunite classes. Similar patterns of minerals were present in the Early Cretaceous rocks in the Kharnak-Kanjar AOI. Kaolinite containing possible dickite is also present within these zones. Visual inspection of the spectra confirmed that variations exist in the kaolinite clay absorption in these areas, but spectra with strong absorption features indicative of abundant dickite or alunite concentrated within pixels were not found in this preliminary analysis. Mineral mixtures of kaolinite with small amounts of dickite and/or alunite are more consistent with the spectra of these pixels. Additional studies of the spectra in these areas should be conducted in conjunction with laboratory spectroscopy and other mineral assays of samples from these areas.

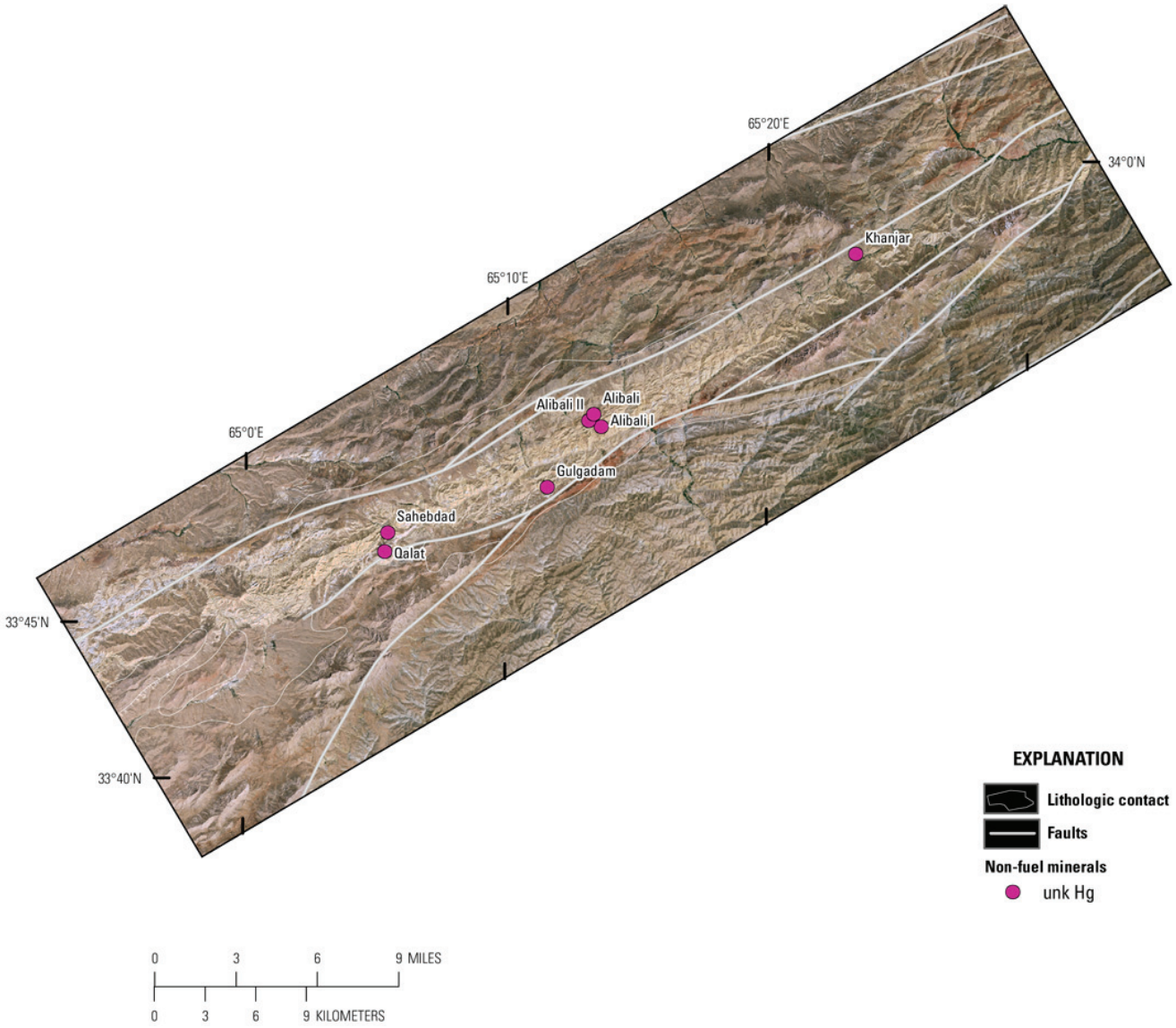

Figure 9B–21. Contrast-enhanced Landsat Thematic Mapper natural-color image of the Sahebdad Khanjar subarea of the Kharnak-Kanjar area of interest. Geologic units and faults from Abdullah and Chmyriov (1977) and Doebrich and others (2006). unk, unknown.

Two minerals, buddingtonite and pyrophyllite, were found that can be formed hydrothermally and are possible indicators of mercury, gold, or silver deposits. Buddingtonite was detected in a mapped unit of Valanginian-Hauterivian Early Cretaceous rocks, with kaolinite and alunite detected along a nearby contact with Pliocene rocks. Because buddingtonite can be indicative of hydrothermal alteration

associated with mercury deposits, additional detailed study of this area including detailed geological mapping, lithologic sampling, and geochemical studies is recommended. An extensive area of pixels was present that matched the spectrum of pyrophyllite, a phyllosilicate that can be formed hydrothermally and is a possible indicator of gold and silver deposits. The spectra were strongly indicative of the mineral and occurred in a spatially contiguous pattern surrounded by pixels matched to spectra of kaolinite and kaolinite mixed with alunite. The main pyrophyllite zone was over 13 km long and up to 7 km wide, and contained within a mapped unit of Valanginian-Hauterivian Early Cretaceous rocks. The spectra of pixels in this area have the strongest alunite absorption features of any pixels matched to this mineral in the Kharnak-Kanjar AOI. Because pyrophyllite can be indicative of hydrothermal alteration associated with metallic ore deposits, additional detailed study of this area relating the spectral identifications to geologic mapping is recommended to determine whether field surveys for lithologic and geochemical sampling are warranted.

Figure 9B–22. Map showing sites of mineralization (Peters and others, 2007) indicated by deposit type in relation to geology of the Sahebdad Khanjar subarea of the Kharnak-Kanjar area of interest. Geology from digital geologic map of Afghanistan (from Abdullah and Chmyriov, 1977; Doebrich and Wahl, 2006; Peters and others, 2007). unk, unknown.

Inspection of the spectra of areas that had scattered pixels matched to serpentine reveal weak features at 2.3 μm, and sometimes at 2.2 μm, with relatively low reflectance levels. The low reflectance level resulted in a relatively low signal-to-noise ratio (S/N) in these pixels, and likely resulted in

misidentification of these pixels as serpentine. In addition, the low S/N may have led to misidentification in pixels adjacent to the serpentine detections. A false-color composite of three HyMap bands (red, green, and blue, loaded with HyMap channels 111, 86, and 6, equivalent to 2.272, 1.738, and 0.542 µm, respectively) highlighted these rocks with purple and blue shading. It is possible that the spectral library does not have a representative entry for the mineral or mineral mixture of rocks in these areas. In general, the reflectance spectra in these pixels bear close resemblance to the spectra of unidentified rocks found in the Panjsher Valley AOI (chap. 13B of this report).

Abdullah and others (1977) describe mercury occurrences as having a stock consisting mainly of calcareous-dickitized metasomatites having variable iron hydroxide content. The minerals detected in the HyMap imaging spectrometer around the known mercury occurrences compare very well with that description. Patterns of kaolinite mixed with calcite and calcite mixed with clay/muscovite, within areas mapped as containing goethite and surrounded by areas containing just calcite are present close to the Kharnak, Pushwara, Duwalak and Surkhnow mineral occurrences in the Koh-e-Katif Passaband subarea, the Khanjar, Qalat, Alibali, Alibali-I, Alibali-II, Gulgadam, and Sahebdad occurrences in the Sahebdad Khanjar subarea, and the Mullayan occurrence in the Pahjshah Mullayan subarea. In all subareas, additional sites with mineral patterns similar to those near mercury occurrences were found distant from the known mineral occurrences. The locations of these areas were identified. In future studies of the Kharnak-Kanjar AOI, these areas should be considered as potential field sampling sites.

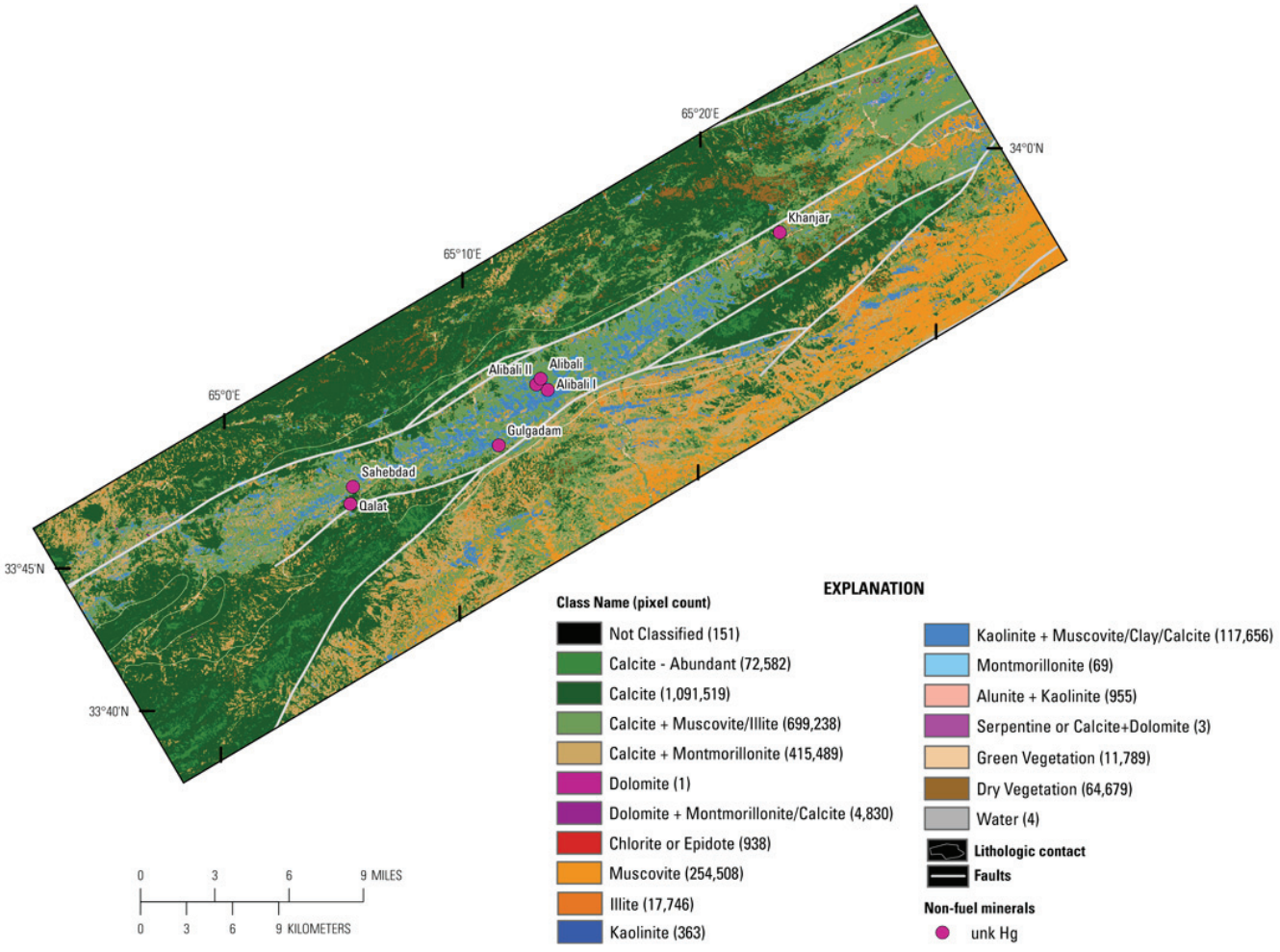

Figure 9B–23. Map showing carbonates, phyllosilicates, sulfates, altered minerals, and other materials derived from HyMap data in the Sahebdad Khanjar subarea of the Kharnak-Kanjar area of interest. unk, unknown.

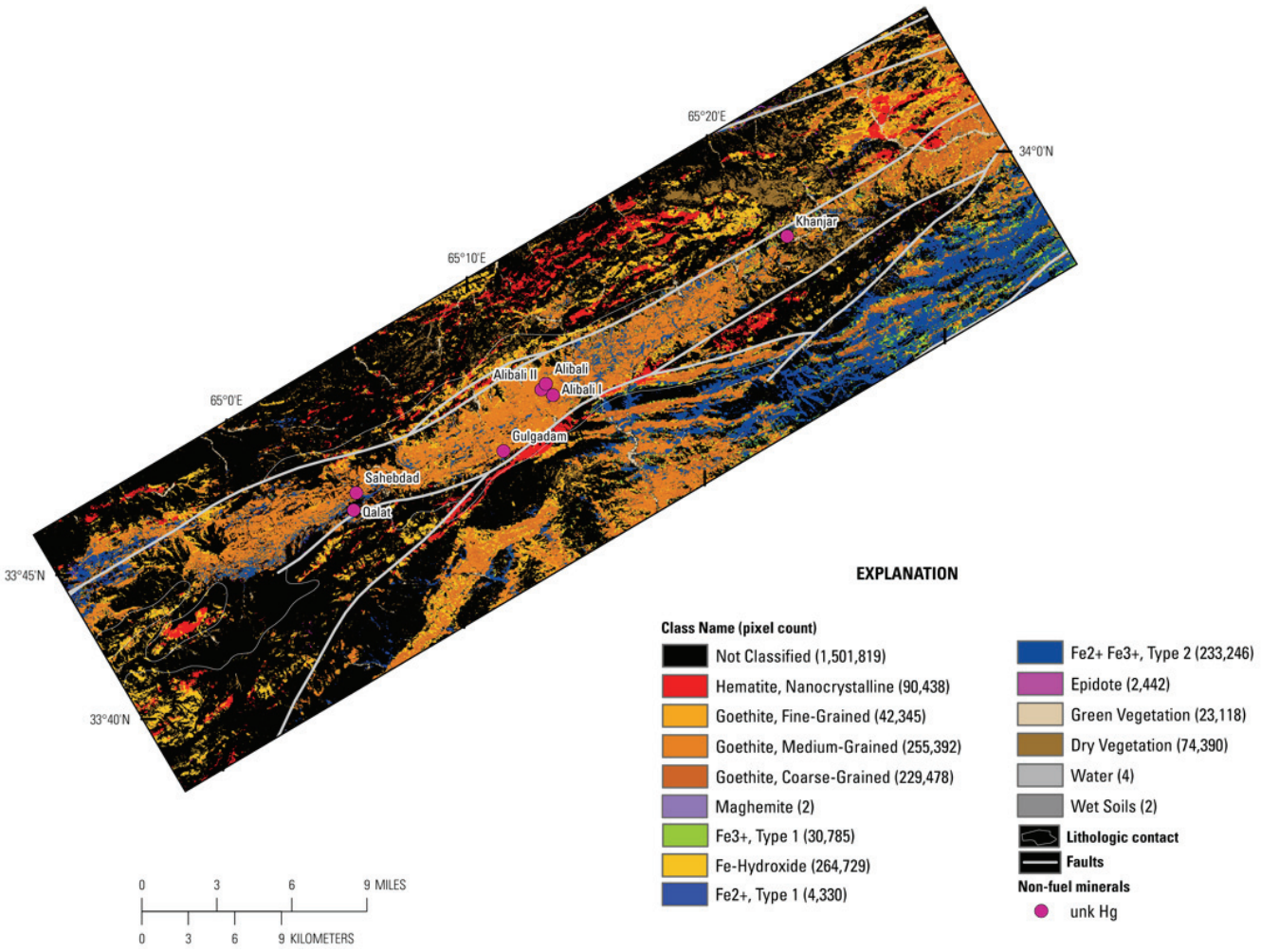

Figure 9B–24. Map showing iron-bearing minerals and other materials derived from HyMap data in the Sahebdad Khanjar subarea of the Kharnak-Kanjar area of interest. unk, unknown.

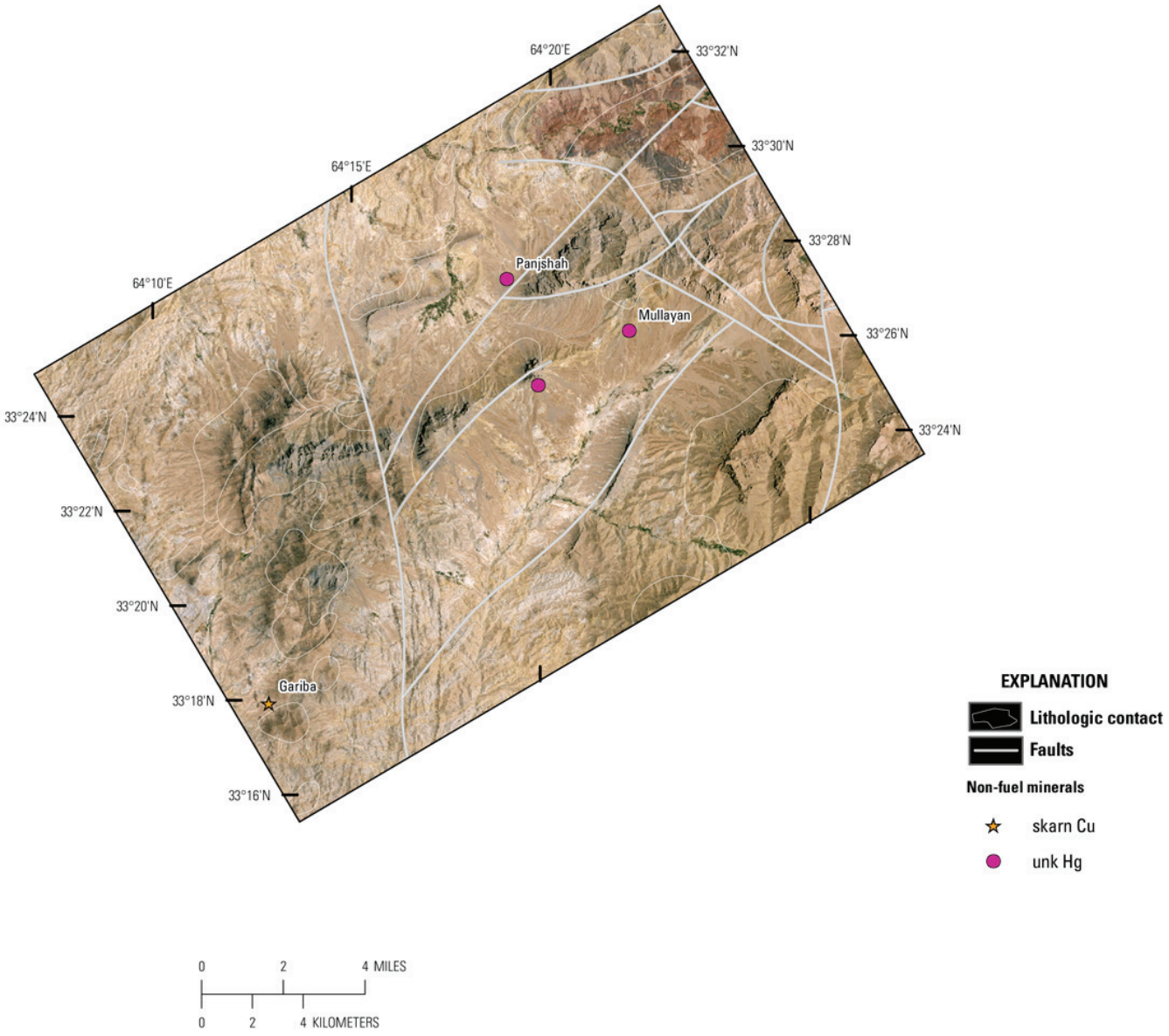

Figure 9B–25. Contrast-enhanced Landsat Thematic Mapper natural color image of the Pahjshah Mullayan subarea of the Kharnak-Kanjar area of interest. Geologic units and faults from Abdullah and Chmyriov (1977) and Doebrich and others (2006). unk, unknown.

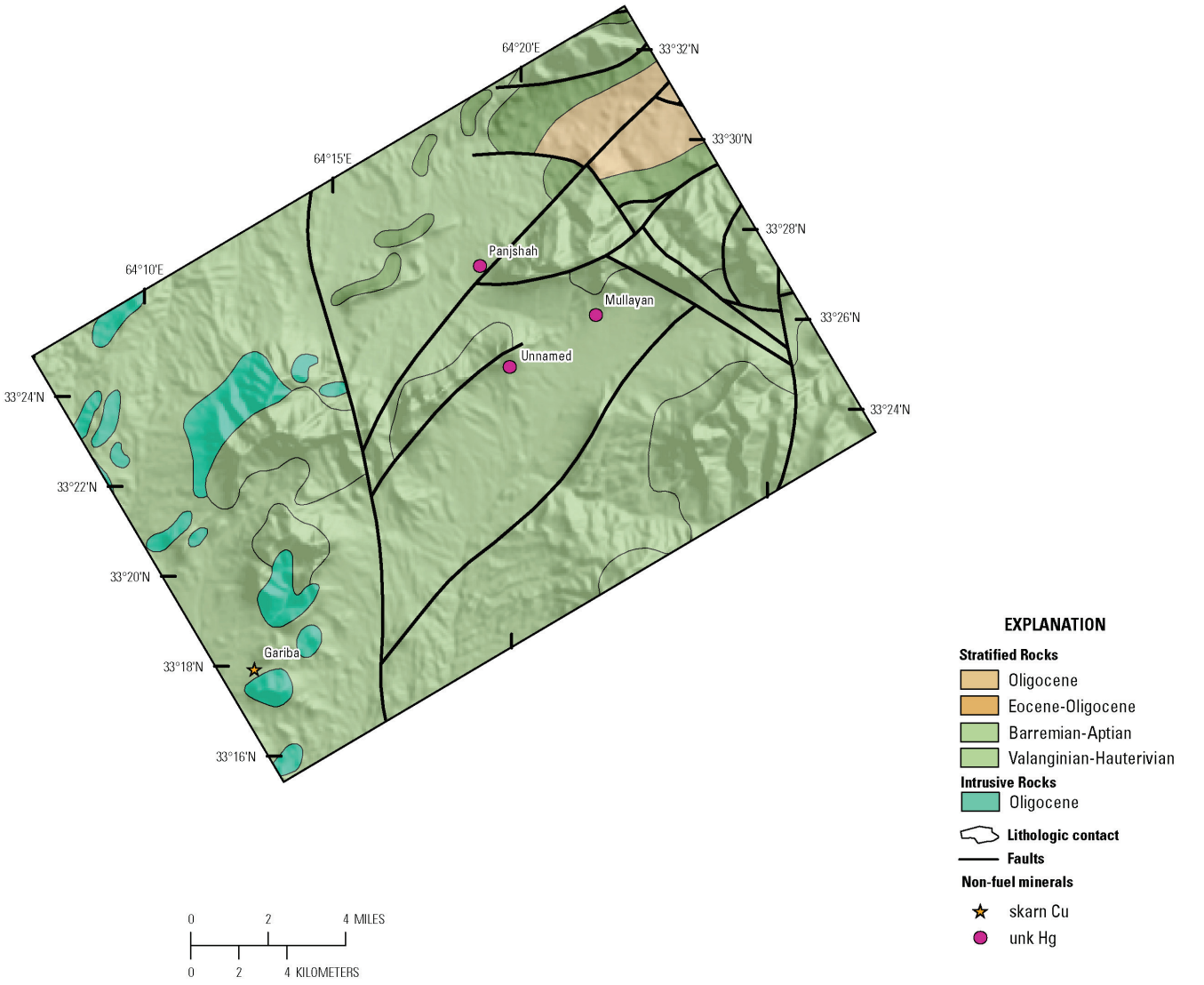

Figure 9B–26. Map showing sites of mineralization (Peters and others, 2007) indicated by deposit type in relation to geology of the Pahjshah Mullayan subarea of the Kharnak-Kanjar area of interest. Geology from digital geologic map of Afghanistan (Abdullah and Chmyriov, 1977; Doebrich and Wahl, 2006; Peters and others, 2007). unk, unknown.

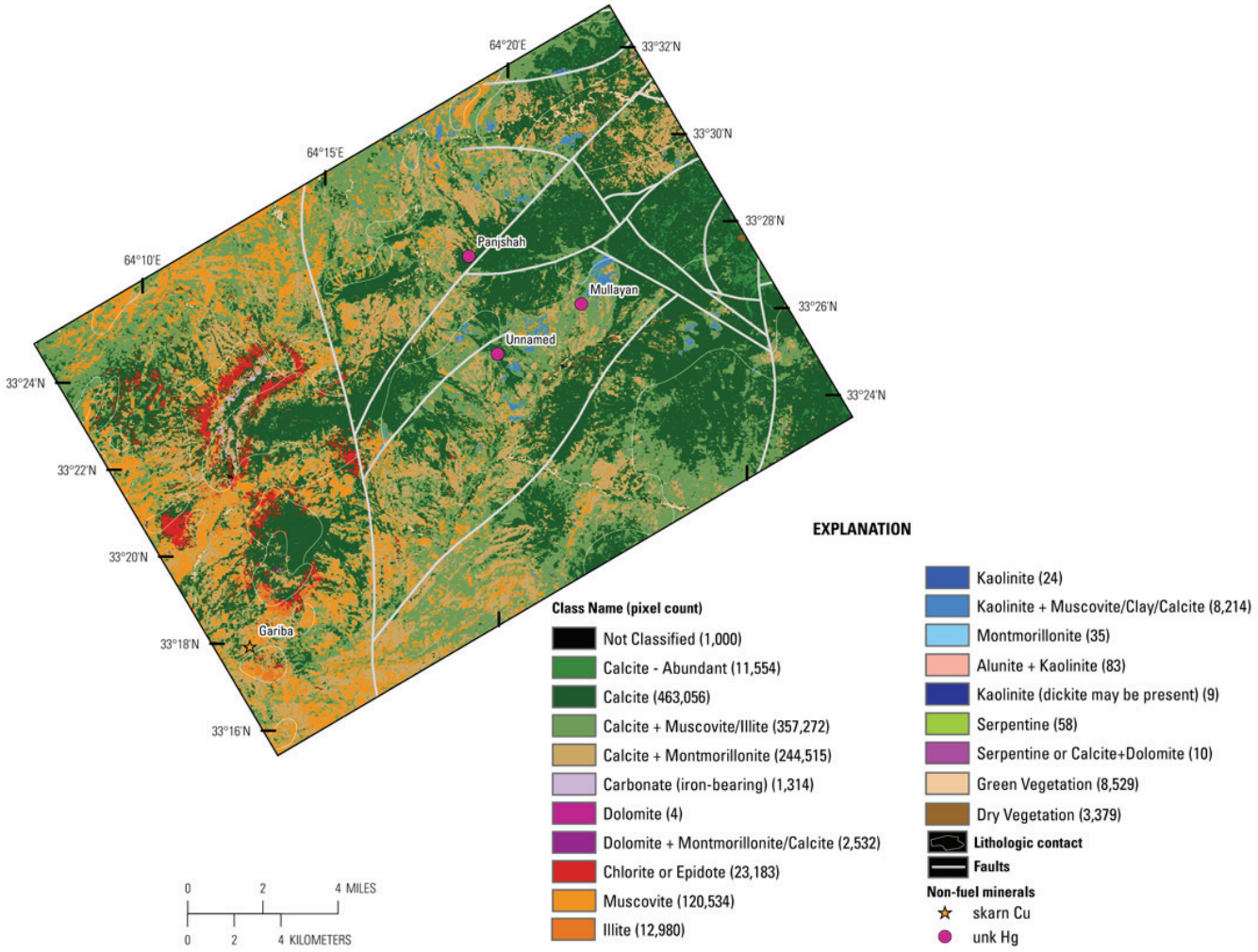

Figure 9B–27. Map showing carbonates, phyllosilicates, sulfates, altered minerals, and other materials derived from HyMap data in the Pahjshah Mullayan subarea of the Kharnak-Kanjar area of interest. unk, unknown.

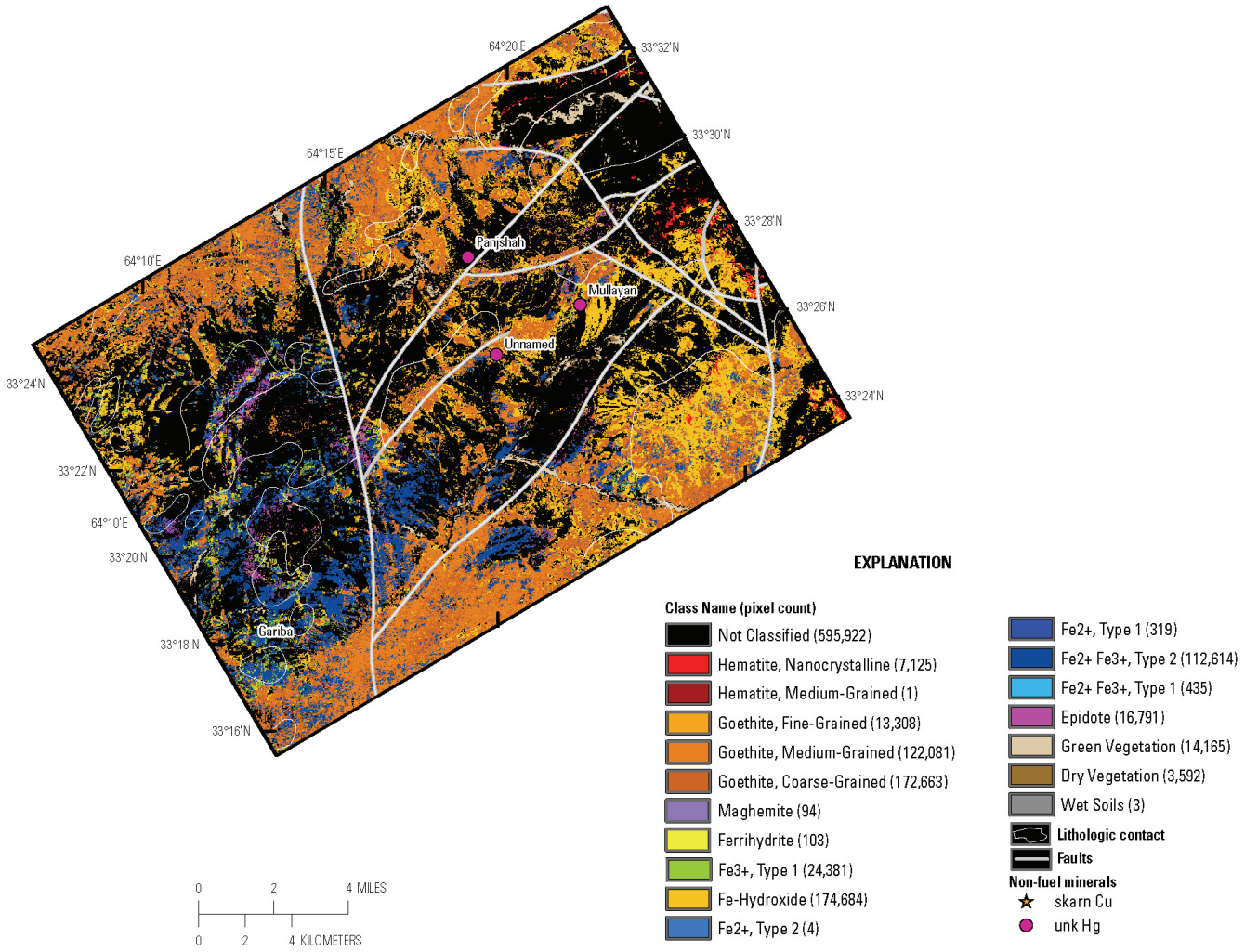

Figure 9B–28. Map showing iron-bearing minerals and other materials derived from HyMap data in the Pahjshah Mullayan subarea of the Kharnak-Kanjar area of interest. unk, unknown.

9B.6 References Cited

Abdullah, Sh., and Chmyriov, V.M., 1977, Geological map of Afghanistan: Kabul, Afghanistan, Ministry of Mining and Industry of the Democratic Republic of Afghanistan, scale 1:500,000.

Abdullah, Sh., Chmyriov, V.M., Stazhilo-Alekseev, K.F., Dronov, V.I., Gannan, P.J., Rossovskiy, L.N., Kafarskiy, A.Kh., and Malyarov, E.P., 1977, Mineral resources of Afghanistan (2d ed.): Kabul, Afghanistan, Republic of Afghanistan Geological and Mineral Survey, 419 p.

Cocks, T., Jenssen, R., Stewart, A., Wilson, I., and Shields, T., 1998, The HyMap airborne hyperspectral sensor—The system, calibration and performance, *in* Schaepman, M., Schlapfer, D., and Itten, K.I., eds., Proceedings of the 1st EARSeL Workshop on Imaging Spectroscopy, 6–8 October 1998, Zurich: Paris, European Association of Remote Sensing Laboratories, p. 37–43.

Davis, P.A., 2007, Landsat ETM+ false-color image mosaics of Afghanistan: U.S. Geological Survey Open-File Report 2007–1029, 22 p. (Also available at *http://pubs.usgs.gov/of/2007/1029/*.)

Doebrich, J.L., and Wahl, R.R., comps., *with contributions by* Doebrich, J.L., Wahl, R.R., Ludington, S.D., Chirico, P.G., Wandrey, C.J., Bohannon, R.G., Orris, G.J., Bliss, J.D., and ___, 2006, Geologic and mineral resource map of Afghanistan: U.S. Geological Survey Open File Report 2006–1038, scale 1:850,000, available at *http://pubs.usgs.gov/of/2006/1038/*.

Hoefen, T.M., Kokaly, R.F., and King, T.V.V., 2010, Calibration of HyMap data covering the country of Afghanistan, *in* Proceedings of the 15th Australasian Remote Sensing and Photogrammetry Conference, Alice Springs, Australia, September 12–17, 2010, p. 409, available at *http://dl.dropbox.com/u/81114/15ARSPC-Proceedings.zip/*.

King, T.V.V., Kokaly, R.F., Hoefen, T.M., and Knepper, D.H., 2010, Resource mapping in Afghanistan using HyMap data, *in* Proceedings of the 15th Australasian Remote Sensing and Photogrammetry Conference, Alice Springs, Australia, September 12–17, 2010, p. 500, available at *http://dl.dropbox.com/u/81114/15ARSPC-Proceedings.zip/*.

King, T.V.V., Kokaly, R.F., Hoefen, T.M., Dudek, K., and Livo, K.E., 2011, Surface materials map of Afghanistan—Iron-bearing minerals and other materials: U.S. Geological Survey Scientific Investigations Map 3152–B.

Kokaly, Ray, 2011, PRISM—Processing routines in IDL for spectroscopic measurements: U.S. Geological Survey Open-File Report 2011–1155, available at *http://pubs.usgs.gov/of/2011/1155/*.

Kokaly, R.F., King, T.V.V., and Livo, K.E., 2008, Airborne hyperspectral survey of Afghanistan 2007—Flight line planning and HyMap data collection: U.S. Geological Survey Open-File Report 2008–1235, 14 p.

Kokaly, R.F., King, T.V.V., Hoefen, T.M., Dudek, K., and Livo, K.E., 2011, Surface materials map of Afghanistan—Carbonates, phyllosilicates, sulfates, altered minerals, and other materials: U.S. Geological Survey Scientific Investigations Map 3152–A.

Peters, S.G., Ludington, S.D., Orris, G.J., Sutphin, D.M., Bliss, J.D., and Rytuba, J.J., eds., and the U.S. Geological Survey-Afghanistan Ministry of Mines Joint Mineral Resource Assessment Team, 2007, Preliminary non-fuel mineral resource assessment of Afghanistan: U.S. Geological Survey Open-File Report 2007–1214, 810 p., 1 CD–ROM. (Also available at *http://pubs.usgs.gov/of/2007/1214/*.)